CHALMERS
UNIVERSITY OF TECHNOLOGY

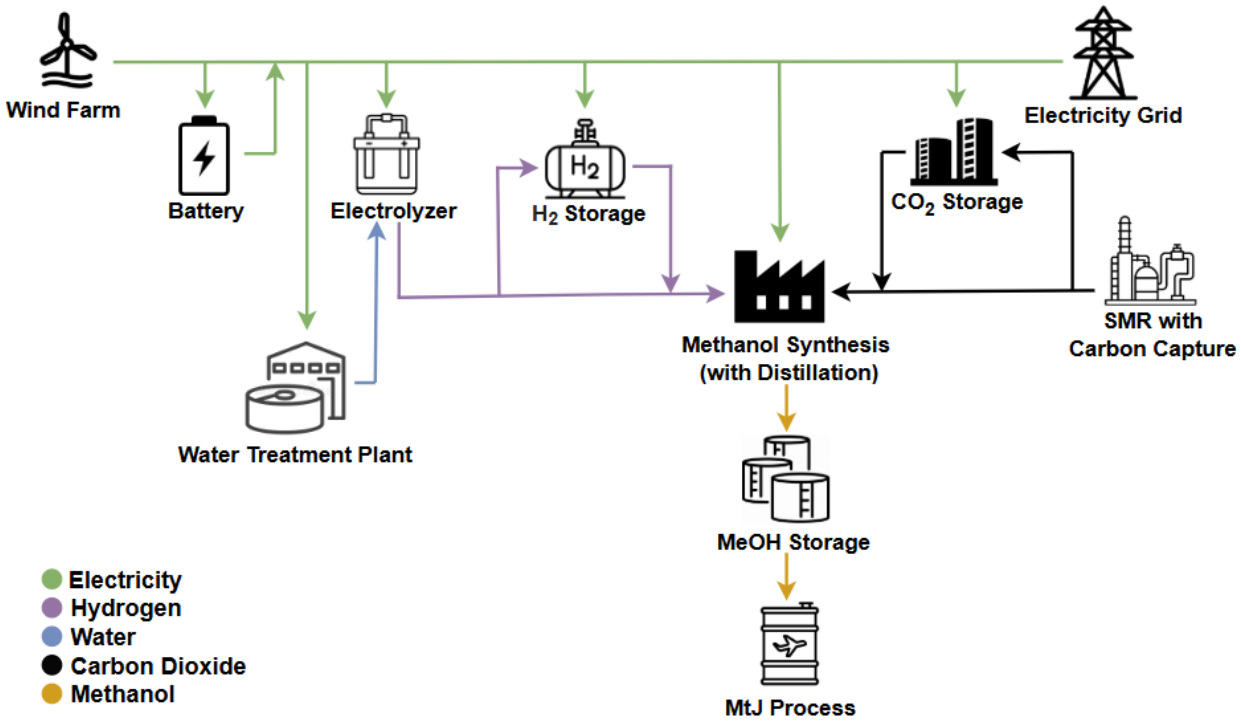

Cost-Optimization and Feasibility of e-Methanol Production Powered by Offshore Wind Energy

Master's thesis in Master Program Sustainable Energy Systems (MPSES)

ARA OMAR
JOHAN WIDGREN

DEPARTMENT OF SPACE, EARTH AND TECHNOLOGY

CHALMERS UNIVERSITY OF TECHNOLOGY
Gothenburg, Sweden 2025
www.chalmers.se

Master's thesis 2025

Cost-Optimization and Feasibility of e-Methanol Production Powered by Offshore Wind Energy

Ara Omar

Johan Widgren

CHALMERS
UNIVERSITY OF TECHNOLOGY

Department of Space, Earth and Environment
Division of Energy Technology
Chalmers University of Technology

Gothenburg, Sweden 2025

Cost-Optimization and Feasibility of e-Methanol Production Powered by Offshore Wind Energy
ARA OMAR & JOHAN WIDGREN

Supervisor: Johanna Beiron, Department of Space, Earth and Environment
Supervisor: Judit Fortet Casabella, Department of Space, Earth and Environment
Supervisor: Kassam Abdel Mallak, Preem

Examiner: Simon Harvey, Department of Space, Earth and Environment

Master's Thesis 2025
Department of Space, Earth and Environment
Division of Energy Technology
Chalmers University of Technology
SE-412 96 Gothenburg
Telephone +46 31 772 1000

Cover: Illustration of the system configuration.

Typeset in LaTeX
Printed by Chalmers Reproservice
Gothenburg, Sweden 2025

Abstract

This study evaluates the technical and economic feasibility of local production of e-methanol as a key component for production of e-Sustainable Aviation Fuel (e-SAF) at Preem's Lysekil refinery in Sweden. The study is driven by the need to decarbonize aviation through electrofuels (RFNBOs) mandated by regulations such as ReFuelEU Aviation, which requires a significant increase in SAF blending by 2050 as well as Preem's 2035 climate neutrality target.

The production system investigated in this work includes water electrolysis powered by renewable electricity, CO_2 from the refinery's existing Steam Methane Reformer (SMR), and methanol synthesis. Electricity is assumed to be purchased from the planned Mareld offshore wind farm through a Power Purchase Agreement (PPA) at a price of 70 €/MWh. Flexibility measures include hydrogen storage (Lined Rock Caverns, LRC), Battery Energy Storage (BES) to manage wind intermittency. Methanol synthesis was modeled in Aspen Plus, while system production costs were minimized using linear optimization tools in GAMS across five scenarios. The results indicate that the cost-optimal electrolyzer capacity ranges from 368–455 MW, and methanol production from 1,288–1386 t/day. LRC-based H_2 storage of up to 28.2 GWh was selected in a wind-powered-only scenario. Tank storage was not included in cost-optimal configurations, although it may be needed in practice. The levelized methanol cost (LCOM) is shown to range from 1592–2157 €/t, and RFNBO-compliant LCOM from 1612-2252 €/t. RFNBO-compliant methanol refers to renewable methanol that meets EU criteria for RFNBOs, which include strict requirements on renewable electricity sourcing and greenhouse gas emission savings. Large-scale H_2 storage offered the largest cost reduction compared to BES. If the facility is able to purchase power from the grid when needed, overall costs are lower, and BES is not necessary. However, such a set-up reduces the fraction of annual production that is RFNBO-compliant, which can potentially affect profitability.

Sensitivity analysis identified electricity price, electrolyzer CAPEX, and electrolyzer efficiency as key cost drivers. Methanol plant flexibility was shown to have a limited impact on cost. H_2 imports from regions or countries with low production costs such as North Africa or Chile could be more economical if PPA prices for off-shore wind-based electricity exceed 30–43 €/MWh. However, imports pose risks related to supply chains, infrastructure, RFNBO policy compliance, and energy security. Importing methanol instead would make a methanol plant in Lysekil redundant. Net Present Value analysis showed high sensitivity to the expected market price for methanol as well as discount rate. Increasing the discount rate from 8% to 12% extends the payback period by approximately 13 years. A 15-year payback was possible for a methanol market price of 1750 €/t, but break-even cannot be achieved at 1250 €/t and 1500 €/t. Local e-methanol production is not currently cost-competitive relative to a forecasted market price of approximately 1300 €/t in 2034, an estimate that remains highly uncertain and depends heavily on the pace of e-fuel deployment. The assumed PPA price of 70 €/MWh remains a critical factor for cost-competitiveness, as achieving profitability would require a significantly

lower electricity price. While large-scale H_2 storage appears cost-optimal, high costs and market uncertainties suggest that import scenarios deserve further analysis.

Acknowledgements

First of all, we would like to thank Kassam Abdel Mallak at Preem for providing us with the opportunity to do our master's thesis at Preem. You have not only given us a lot of input, data, and knowledge about this project, but also regarding refineries and the petrochemical industry in general. You have made this work very fun, and thanks for bearing with us and all of our questions. Kassam, you made this really fun! We would like to thank Johanna Beiron for being so enthusiastic, critical, and always there for us when questions arose. You have been very supportive during our thesis work and made our thesis enjoyable. Thanks to Judit Fortet Casabella for helping us with Aspen Plus and all the discussions regarding methanol synthesis theory vs. process simulation. You rock! We would like to thank Sofia Rosén for being very helpful with the GAMS modeling and guidance, saving us a lot of time. Thank you, Simon Harvey, for the valuable insights and feedback provided throughout this thesis. Being able to have your expertise on this project was greatly appreciated. Lastly, we are very thankful for the world-class wind data that Niclas Mattsson provided us with to make our modeling complete.

Ara Omar & Johan Widgren, Gothenburg, May 2025

List of Acronyms

Below is the list of acronyms that have been used throughout this thesis listed in alphabetical order:

AWE	Alkaline Water Electrolysis
BES	Battery Energy Storage
CO_2	Carbon Dioxide
CO	Carbon Monoxide
DAC	Direct Air Capture
GHG	Greenhouse Gas
H_2	Hydrogen Gas
LCOE	Levelized Cost of Electricity
LCOH	Levelized Cost of Hydrogen
LCOM	Levelized Cost of Methanol
LRC	Lined Rock Cavern
MtJ	Methanol-to-Jet Fuel
NPV	Net Present Value
PEM	Proton Exchange Membrane Electrolysis
PPA	Power Purchase Agreement
RED	Renewable Energy Directive
RFNBO	Renewable Fuels of Non-Biological Origin
SAF	Sustainable Aviation Fuel
SMR	Steam Methane Reformer
SOEC	Solid Oxide Electrolysis
TRL	Technology Readiness Level

Contents

List of Acronyms **xi**

List of Figures **xv**

List of Tables **xvii**

1 Introduction **1**
1.1 Purpose and Aim of Study 4

2 Theory **5**
2.1 Methanol Synthesis 5
2.2 Electrofuels 6
2.3 RFNBO Requirements 7
2.3.1 Power Purchase Agreement 8
2.4 Overview of e-methanol Production System 9
2.5 Hydrogen Production via Electrolysis 10
2.6 Energy Storage Options as Flexibility Measures 10
2.6.1 Hydrogen Storage 10
2.6.2 Batteries 11
2.6.3 CO_2 Storage 12

3 Methods **13**
3.1 Methanol Synthesis Process Modeling 13
3.2 Estimation of Compression Work 16
3.2.1 Hydrogen Compression 16
3.3 Linear Optimization Model 16
3.3.1 Objective Function 20
3.3.2 Model Constraints 21
3.3.2.1 Technology Constraints 21
3.3.2.2 Storage Dynamics 22
3.3.2.3 Electricity Balance 23
3.3.2.4 Emissions Calculations 24
3.4 Key Performance Indicators 24
3.5 Case Study 26
3.6 Scenarios 28

4 Results **31**

4.1 Aspen Modeling Results 31
4.2 Overview of Cost-Optimal System Results 32
4.3 Value of Flexibility Measures and Feasibility 34
4.4 Technical Potential to Reduce Costs 38
4.4.1 Electrolyzer Efficiency and CAPEX 38
4.4.2 Alternative Electrolyzer Technologies 39
4.4.3 Methanol Synthesis Flexibility and Conversion Efficiency . . . 40
4.5 Sensitivity to Intermittency and Electricity Costs 41
4.6 Import in the Supply Chain 43
4.7 Economic Feasibility and Competitiveness 45

5 Discussion **49**
5.1 Market Uncertainties 49
5.2 Energy Security 50
5.3 Policy Barriers and Opportunities 51
5.4 Import and International Production 51
5.5 Further Work Suggestions 52

6 Conclusion **53**

A Compression work **I**

B Wind Data **III**

C Electrolyzer technologies **V**

List of Figures

1.1 Sustainable aviation fuel (SAF) and RFNBO mandates required by ReFuelEU Aviation. 1

2.1 Visualization of e-methanol system considered in this study. 9

3.1 Illustration of methodology approach. 13
3.2 Methanol Synthesis flowsheet created in Aspen Plus. 14
3.3 Simplified system boundary of the case study. 26

4.1 Results from Aspen simulation of methanol synthesis. 31
4.2 Sankey diagram of energy flows and losses in *Full Flex* scenario. . . . 33
4.3 Resulting annual cost distribution of system in the *Full Flex* scenario. 34
4.4 Cost distribution of resulting LCOM in each scenario. 36
4.5 Cost distribution of resulting LCOH in each scenario. 37
4.6 Resulting impact on $LCOM_{RFNBO}$ from the varying of PEM efficiency and CAPEX in the *Full Flex* scenario, where the red dot represents the base case. 38
4.7 Resulting impact on $LCOM_{RFNBO}$ from the varying of electrolyzers types, efficiency and CAPEX in the *Full Flex* scenario. 39
4.8 Resulting impact on $LCOM_{RFNBO}$ from the varying of ramp rates and minimum load for the methanol synthesis plant in the *Full Flex* scenario. 40
4.9 Resulting impact on $LCOM_{RFNBO}$ from varying electricity price and wind capacity factors (CFs) in the *Full Flex* scenario. 42
4.10 Cost comparison between importing hydrogen or local production through varying PPA price, along with the effect on $LCOM_{RFNBO}$. . 44
4.11 NPV curve of the project in the *Full Flex* scenario, based on different e-methanol prices. 46
4.12 NPV curve of the project in the *Full Flex* scenario, based on different discount rates. Market price set to 1750 €/t 47

B.1 Illustrations of the Mareld wind farm region and corresponding wind data region. III
B.2 Power curve for Vestas V-236 15MW wind turbine, assumed to be used at Mareld wind farm. IV

List of Tables

3.1 Description of sets and variables used in GAMS modeling. 17
3.2 Description of technical properties for storage technologies, used as parameters in GAMS modeling. 18
3.3 Description of technical properties for generating technologies, used as parameters in GAMS modeling. 19
3.4 Additional parameters used in GAMS modeling. 19
3.5 Visualization of flexibility measures available in each scenario. 29

4.1 Calculated and converted Aspen modeling results for GAMS modeling. 32
4.2 Full Flex results. 33
4.3 Overview of notable installed capacities of storage and technology units, in each scenario 35
4.4 Resulting KPIs for each scenario 37

A.1 Parameter values and result from H_2 compression calculations I

C.1 Parameter values used in sensitivity analysis for different electrolyzers V

1
Introduction

In the coming years, sectors such as shipping, aviation, and the chemical industry must significantly reduce their fossil carbon dioxide (CO_2) emissions to comply with emission reduction targets to reach net-zero CO_2 emissions by 2050 [1]. For these sectors, substitution of fossil fuels by direct electrification is not a feasible solution in the near future [2]. However, renewable alternatives exist that can help decarbonize heavy transport and the chemical industry substantially [2]. The rapid implementation of *electrofuels* (also called *synthetic fuels*) is one way to contribute to the decarbonization of the transport sector [3]. To incentivize emission reductions in the hard-to-abate sectors such as aviation, EU has established an initiative called *ReFuelEU Aviation*, which outlines a gradual increase in the share of *sustainable aviation fuels* (SAFs) in the blending mix at EU airports [4]. As of 2025, the share of SAF in aviation fuel is required to be 2 % and by 2050, 70 % [5] (See Figure 1.1). SAF is a jet fuel made from non-fossil feedstocks and can be produced from for example waste, biomass and fats/oils [6]. The fuel can be blended with conventional aviation fuel, thereby reducing emissions up to 90% (if fully blended), compared to fossil-based fuel [7].

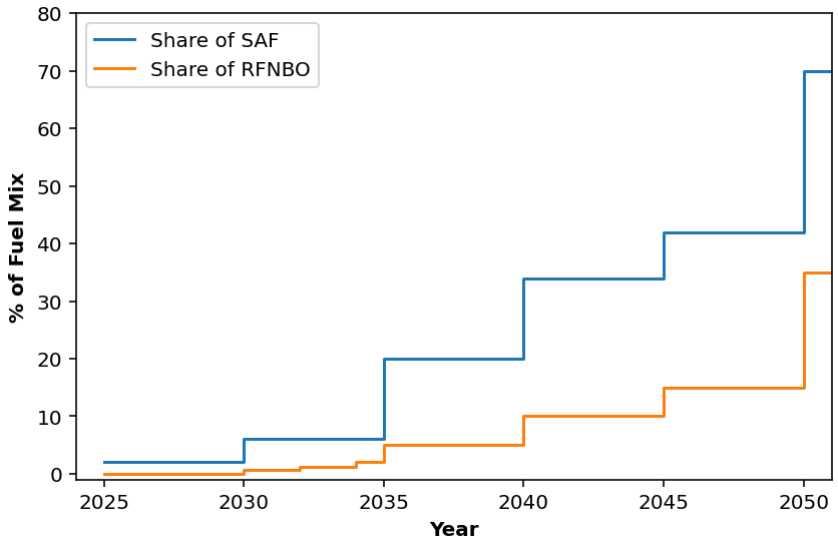

Figure 1.1: Sustainable aviation fuel (SAF) and RFNBO mandates required by ReFuelEU Aviation.

ReFuelEU Aviation defines SAF as a collective term for aviation fuels that do not

use fossil carbon, categorizing them into four different types based on their carbon feedstock [8]. However, only one of these, *synthetic aviation fuels* (also known as *Renewable Fuels of Non-Biological Origin (RFNBOs)*), is explicitly required to increase in share within total aviation fuel under the ReFuelEU Aviation policy [9]. RFNBO is defined by the Renewable Energy Directive (RED III) as a fuel derived from renewable hydrogen (H_2) and captured CO_2 from industrial processes, Direct Air Capture (DAC) or biogenic CO_2. [8], [10].

One way to produce synthetic aviation fuel is to first react H_2 and CO_2 to synthesize methanol, followed by upgrading the methanol to jet fuel in a methanol-to-jet process. Methanol is a very versatile platform chemical that can be used in several sectors, such as transportation, chemical and electricity generation [11]. Most methanol is currently produced from natural gas, but if produced via renewable feedstock, the carbon emission reduction can be above 90 % [12]. Since conventional methanol already has a well-established infrastructure for production, storage, and distribution, it can potentially be integrated into existing systems more easily compared to some other electrofuels. Although E-methanol offers a viable path for emission reductions in hard-to-abate sectors, the main challenge is still the high production cost compared to fossil methanol [13].

There are currently several projects within this field, where Liquid Wind is a frontrunner for e-methanol production, utilizing biogenic CO_2 captured from power generation and renewable energy from wind power. However, no large-scale plants are in operation yet, except for a plant in Kassø, Denmark, that uses solar PV to produce renewable H_2 and biogenic CO_2 from biogas production. As of March 2025, Kassø has been certified and is the first of its kind for RFNBO methanol production [14]. According to Hydrogen Europe, only one batch of *green* H_2 (H_2 produced from renewable electricity) has been produced at the site [15]. Generally, there are challenges with profitability, hence most large e-methanol projects are currently being postponed or canceled [16],[17].

Preem, the largest petroleum refiner and transport fuel producer, and one of the largest liquid biofuel producers in Sweden, has publicly stated that their ambition is to transition towards becoming climate-neutral across the whole supply chain by 2035 [18],[19], [20]. Preem has two refineries located on the west coast of Sweden, in Gothenburg and Lysekil. They are both regarded as two of Europe's most up-to-date refineries, with their combined operation accounting for roughly 80 % of the Swedish refinery capacity as well as 40 % of Nordic production [21]. Preem has already invested towards increasing their sustainable fuel production at the Lysekil refinery, enabling almost 2 million m^3 of renewable fuel yearly by 2029, including SAF [22]. In year 2029, 600 000 m^3 SAF will be produced annually, which accounts for the entire domestic aviation demand [22]. While the notable strides have been in renewable road transport fuels, they are also planning to investigate in the economic viability of investing in the development of *Electro-Sustainable Aviation Fuel* (e-SAF) for implementation within the next decade, where e-methanol is a crucial building block [2], [23], [24].

The aim of this project is to contribute to this endeavor by investigating the technical and economic viability of e-SAF production. The supply chain proposal is assumed to begin with the utilization of the favorable offshore wind conditions of the coastal area outside Lysekil to produce green H_2. By combining H_2 with CO_2 captured from a *steam methane reformer* (SMR) at the refinery site, an intermediary product for the e-SAF synthesis, e-methanol (e-MeOH) , can be produced through a carbon-neutral process. The methanol produced at the refinery site can then be further processed to produce e-SAF through a methanol-to-jet (MtJ) process.

However, timing the transition to e-SAF presents significant challenges, particularly in the supply-demand aspect [25]. The supply cannot meet the current fuel demand of SAF at the moment [26]. The scarcity of SAF along with the sensitive nature of refinery operating costs and high production costs are the reasons why the price of SAF is much higher than for conventional jet fuel [25]. The general consensus in the literature is that, due to the high electricity demand, one of the primary ways to reduce operational costs is to use cheaper electricity, which in the case of renewables like wind and solar, are directly dependent on weather conditions, making regions with favorable capacity factors appealing. Additionally, to mitigate risks, the producer would need to acquire offtake agreements, by securing a contract for a certain volume of SAF, reducing the risk for the producer (in this case Preem) and the buyer (airline or airport) [27]. Therefore, this project will not only look into the design of such a system and technical constraints, but also the economic aspect of the production system to minimize the cost of e-methanol. The production cost will also be compared to scenarios of H_2 import to evaluate the cost-effectiveness.

Previous studies have investigated different aspects such as system configurations and economic viability of methanol production. Before Kassø was put into operation, a study was conducted for the plant to investigate the impact of intermittent energy (solar power) and its impact on both the economic and performance of the plant. It was concluded that the intermittent output of the solar plant significantly influenced both the performance and the economic feasibility [28]. Another study investigated a combined energy system, supplying energy from wind, solar PV and a CHP plant to produce methanol. However, their conclusion was that in order to achieve cost-competitiveness against fossil-derived methanol, the cost of emitting CO_2 needs to be above 200 €/t [29]. Because of these different challenges, this study will look into a local large-scale e-methanol production system on the west coast of Sweden and how to optimize unit capacities, the potential of importing parts of the supply chain to see if it can reach cost-competitiveness compared to current and projected market prices. The case study assumes that the hydrogen is produced through electrolysis powered mainly by an offshore wind farm located outside Lysekil through a Power Purchase Agreement (PPA).

1.1 Purpose and Aim of Study

The purpose of this thesis is to evaluate the technical and economic feasibility of local e-methanol production as a part of an e-SAF supply chain. The study will aim to identify a viable supply chain and optimize the system design for minimal total costs on a yearly basis while reaching a production goal.
The specific objectives of the project are as follows:

- Evaluate the potential for cost-effective methanol production by optimizing unit capacities and operational parameters across the supply chain, integrating hydrogen production via electrolysis, offshore wind power, cryogenic CO_2 capture, and methanol synthesis.
- Evaluate the technical and economic feasibility of local large-scale methanol production as part of an e-SAF supply chain while investigating whether part or the entire supply chain could be more cost-effective if produced elsewhere.
- Assess the viability and impact of incorporating flexibility measures, including hydrogen storage systems, lithium-ion batteries, and flexible operation modes, at crucial points in the supply chain (such as hydrogen production, energy storage, and methanol synthesis), on the overall system performance and cost-effectiveness.
- Conduct a sensitivity analysis to identify critical parameters that impact system performance and cost-effectiveness and propose strategies for adjusting these parameters to achieve a more robust system design.

2
Theory

This section includes an overview of electrofuels, requirements to produce synthetic aviation fuel, costs, different feedstocks going into the process, and subsystems used in this thesis.

2.1 Methanol Synthesis

Methanol (CH3OH), the simplest alcohol, is considered one of the most versatile basic compounds and an intermediary building block in everyday products, including plastics, paints and more complex fuels [30]. Roughly 100 Mt is produced annually, and production capacity exceeds 150 Mt/a, with most of the methanol being produced from fossil feedstock [31]. There are several pathways to produce methanol, but today, methanol is mainly commercially produced from synthesis gas, a $CO/CO_2/H_2$ mixture, typically derived from natural gas via Steam Methane Reforming (SMR) or from coal through Coal Gasification, respectively [32].

In recent decades, the urgent need for climate action and the emergence of CO_2 mitigation policies have drawn increased attention to an alternative reaction pathway: direct hydrogenation of CO_2 to methanol. This process involves several reactions that can be optimized to convert emissions into renewable methanol. The methanol synthesis can be represented by the following 3 equilibrium reactions:

$$\underset{\text{Methanol Synthesis from } CO_2}{\mathrm{CO_2 + 3\,H_2 \rightleftharpoons CH_3OH + H_2O}} \tag{2.1}$$

$$\underset{\text{Reverse Water Gas Shift (RWGS) Reaction}}{\mathrm{CO_2 + H_2 \rightleftharpoons CO + H_2O}} \tag{2.2}$$

$$\underset{\text{Methanol Synthesis from CO}}{\mathrm{CO + 2\,H_2 \rightleftharpoons CH_3OH}} \tag{2.3}$$

A catalyst is required to react the CO_2 into a methanol product due to CO_2 being a highly stable molecule. The most widely used catalyst in industry is a so-called CZA material, a mixture with differing shares of Cu, ZnO and Al_2O_3 [33]. Apart from catalyzing the key reactions above, the utilization of a copper-based catalyst also suppresses methane and higher hydrocarbons from becoming favorable products under certain reaction conditions, resulting in a product stream with minimal impurities [34]. The synthesis of methanol proceeds more efficiently via 2.1 rather than 2.3 due to the abundance of CO_2, leading to a significant water accumulation

at the outlet. This excess water reduces catalyst lifetime and activity, restricts the reaction, and necessitates an additional distillation step at the end of the process [35].

The equilibrium conversion of the reaction over a CZA catalyst varies with temperature, reaching a maximum at an intermediate temperature, then decreasing at both lower and higher temperatures [34]. With the reactions 2.1 and 2.3 being exothermic, the equilibrium shifts towards the reactants as heat is released during reaction, resulting in higher temperatures which favors the endothermic RWGS reaction 2.2, producing more CO and reducing the selectivity for methanol [36]. However, the reaction is preferably not run at low temperatures, as the catalytic effect of the CZA catalyst is greatly diminished, resulting in the kinetics of methanol synthesis becoming too low.

It is also well established that the methanol synthesis reaction 2.1 is favored at higher pressures, with the limiting factor being feasibility and costs. This is mainly due to Le Chatelier's principle, since the reaction involves the reduction of 4 moles of reactant to 2 moles of product, the reaction will shift to the right in order to reduce the pressure [37]. Additionally, several studies have investigated and modeled the increase of the hydrogen ratio from the stoichiometric ratio in reaction 2.1, and motivating how that can achieve near perfect carbon conversion and methanol selectivity [34]. However, in power-to-methanol schemes, where hydrogen is obtained through electrolysis, the cost of hydrogen is significantly more expensive than conventional hydrogen production through SMR. As such, the stoichiometric ratio in the composition feed is not often pertinent.

This in turn results in the methanol synthesis reaction being an equilibrium reaction where strict reaction conditions, lower temperatures, and higher pressures favor methanol formation, but with the notable downside of very slow reaction rates and methanol selectivity below 200^oC. As such, scientific studies has reached the consensus that the reaction should be conducted strictly and maintained within the 200-250^oC and 10-100 bar range, to ensure highest rate and selectivity [38]. But even under these conditions, the single pass conversion remains low compared to conventional methanol formation through synthesis gas, due to significant buildup of H_2O and exothermic heat. As such it is important and effective to implement an efficient way to remove the heat from the reactor continuously through a coolant, as well as a recycling path for unreacted reactants after a thorough removal of products to avoid accumulation in recycling loops [35].

2.2 Electrofuels

Replacing current fossil fuels with electrofuels could potentially reduce greenhouse gas emissions by more than 50 %, depending on the source of electricity, CO_2 and H_2, and associated production technologies [39].

However, the main challenge regarding electrofuels is the cost, because of the large cost of producing hydrogen through electrolysis. For example, the cost of e-gasoline

is between 1.5 and 2.2 times higher compared to fossil gasoline [40]. For e-methanol, the cost difference is even higher, where industry estimates say that e-methanol from renewable energy and captured CO_2 could cost 2-5 times the cost of conventional methanol [41]. The current methanol prices vary across the globe, with China being the cheapest and Europe the most expensive at 370 and 700 € per ton, respectively [42]. However, implementing policy instruments such as emission costs for natural gas-derived methanol, could potentially make e-methanol cost-competitive by 2040 [43].

2.3 RFNBO Requirements

For the e-methanol to be classified as RFNBO (Renewable Fuels of Non-Biological Origin), certain requirements set by the ReFuelEU Aviation framework must be fulfilled. According to the EU's definition of RFNBO, the feedstocks used in production must be renewable and of non-biological origin, explicitly excluding biomass as an energy feedstock option [44]. In this case study, H_2 produced from renewable sources (such as wind power) and captured CO_2 are used, fulfilling the non-biological origin requirement. This is because the CO_2 feedstock does not add any heating value to the fuel. Additionally, up until 2036 (for CHP plants) and 2041 (for other industrial processes), utilizing captured CO_2 coming from fossil or biogenic sources is allowed, since it does not add energy to the produced fuel. By 2041, captured biogenic CO_2 and DAC will be the only sources that meet the RFNBO criteria [10]. As of 2023, the greenhouse gas emissions savings from RFNBO should be at least 70 %. As outlined in Commission Delegated Regulation (EU) 2023/1185 [45] *All renewable liquid and gaseous transport fuels of non-biological origin and recycled carbon fuels, the total emissions from the fossil fuel comparator shall be 94 gCO2eq/MJ.* This means that to comply with the requirement, the total emissions from the use of RFNBO cannot exceed 28 gCO2eq/MJ (or 100.8 gCO2eq/KWh).

The RFNBO Delegated Act establishes further requirements for electricity used in fuel production. According to the RED regulations, the electricity used for the production of RFNBO must either come directly from a renewable energy production facility or be accompanied by certificates guaranteeing the renewable origin of the electricity. The fuel producer can have renewable energy installations on-site, but if not, the producer must contract one or more power purchase agreements (PPAs) with renewable electricity producers (see section 2.3.1). If the electricity is sourced from the grid, additional steps must be taken to ensure that the renewable share is accurately accounted for [44]. Specifically, the average annual renewable share of the electricity must be measured two years prior to the current year, ensuring compliance with the directive. If electricity taken from the grid is not counted as fully renewable, only the proportion corresponding to the renewable share of the grid mix within the bidding zone will be counted towards the produced RFNBO.

An additional condition, according to the RED article 3, is that the renewable

electricity production unit must either be directly connected to the fuel production site or occur within the same facility. This ensures that the electricity used for RFNBO production is fully renewable. The wind farm can either be connected to the grid or not, but if it is, it must measure the electricity flow to ensure that no electricity has been taken from the grid for RFNBO production. Additionally, the renewable power plant must be operational not earlier than 36 months before the fuel production plant starts, ensuring a reliable energy supply [44].

As mentioned previously, there are additional requirements if electricity is taken from the grid to ensure that it is fully renewable. If the fuel producers have renewable power purchase agreements directly or via intermediaries with renewable electricity producers for an amount at least equivalent to the claimed renewable electricity, fulfills the geographical, temporal correlation, and is located in a bidding zone where the emission intensity of electricity is lower than 5 gCO2eq/kWh it can be considered for RFNBO. The Preem Lysekil refinery, in focus in this work, is located in the bidding zone SE3, which means that the emission intensity criteria are met (2.44 gCO2eq/kWh for SE3), however, grid transmission capacity limits the energy that can be supplied. Therefore a renewable energy plant, such as a wind farm, can mitigate this issue by supplying enough energy. To overcome this bottleneck, installing renewable energy plants such as an offshore wind farm can help ensure a sufficient energy supply throughout the year via PPAs.

The temporal correlation implies that the production must correspond to what is supplied through the renewable power purchase agreements hourly. However, the grid's spot price may also be considered to satisfy the criteria. If the electricity price is below 20 €/MWh or 0.36 times the price of a carbon permit [44], it also complies with the requirements. Lastly, the geographical correlation must simultaneously be met, which is to either be located in the same bidding zone (SE3) or an interconnected zone (SE2, SE4). The geographical correlation can also be achieved by having a PPA from an offshore bidding zone, however none such exist as of May 2025. However, it will not be investigated further in this work.

2.3.1 Power Purchase Agreement

A PPA is a long-term agreement regarding power purchase between a power producer and a power consumer [46]. The purpose is to secure electricity supply at a fixed price and simultaneously reduce/eliminate the potential risks for the investor of the power generation [47]. One advantage of having this type of agreement is to avoid the price volatility of the electricity market. Today, there are several different types of PPAs, and they can be customized according to the customer's needs [48].

Pay-as-Produced PPA has been assumed in the study to fulfill the temporal requirements for RFNBO [44]. Pay-as-Produced is created in a way that favors the inherent variability of renewable energy sources, where the energy producer delivers what is generated instead of a fixed amount [49]. This means that the total energy delivered yearly can be well predicted, but the drawback is that there is

uncertainty on a more detailed timescale. The energy delivered from the wind farm is assumed to be directly connected to the refinery through a transmission line. Additionally, PPAs must be signed with electricity producers within the same bidding zone. While a PPA with a producer in an adjacent bidding zone is allowed, it comes with additional requirements [44].

2.4 Overview of e-methanol Production System

Figure 2.1 gives an overview of the studied system design for the methanol synthesis. The system consists of a wind farm supplying electricity to an electrolyzer, battery storage, and other processes that require electricity to operate at site-specific pressures. The electrolyzer produces H_2 from the electricity, to be stored or utilized directly in the methanol production. The H_2 storage icon in figure 2.1 represents both lined rock cavern (LRC) and tank storage possibilities. The methanol synthesis simultaneously also receives CO_2 (in liquid form, from the cryogenic carbon capture of the SMR) as an input with a specified H_2 and CO_2 ratio to ensure full conversion of the feedstocks to methanol. The crude methanol then gets stored or transferred to the distillation columns, where it is separated from water and purified to reach methanol AA grade, which is an industry purity standard of 99.85 % methanol in weight percentage. The methanol is then stored in tanks on-site to later be used in the *Methanol-to-Jet Fuel* (MtJ) process, where the final product will be RFNBO classified aviation fuel (e-SAF). However, this study's boundaries are up until the MtJ and will not investigate how to operate the MtJ plant.

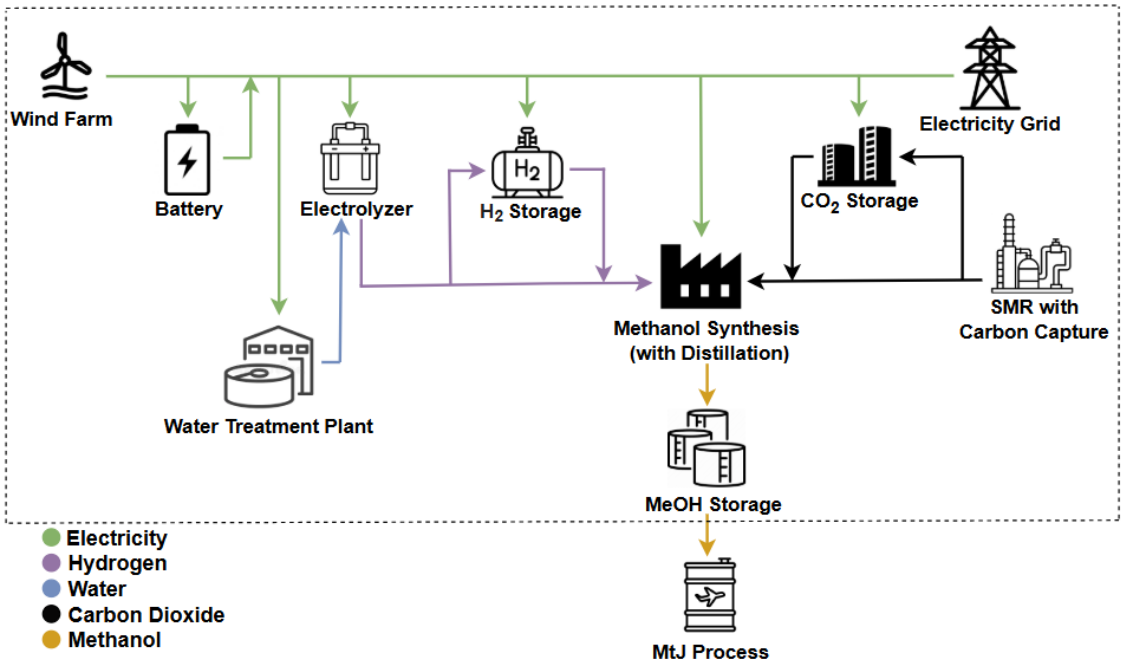

Figure 2.1: Visualization of e-methanol system considered in this study.

2.5 Hydrogen Production via Electrolysis

In principle, water electrolysis is the process by which water molecules are split into hydrogen and oxygen molecules by supplying electricity and water as input [50]. As of today, three considerable types of electrolyzers are either currently commercialized or could be commercialized shortly. These three types are Alkaline Water Electrolysis (AWE), Proton Exchange Membrane Electrolysis (PEM) and Solid Oxide Electrolysis (SOEC). The first two ones are the most mature, demonstrated in practice, and the ones considered when forecasting the development and cost reductions in water electrolysis to produce *green hydrogen* [51].

The methanol production will be influenced by the wind energy generated, so the flexibility of the electrolyzer is necessary. The electrolyzer needs to handle load flexibility. Only PEM is fully flexible when it comes to load variation and has the fastest start-up capabilities [52]. When operating a PEM electrolyzer, heat is generated, which is necessary to cool/remove to not damage the membrane of the electrolyzer [53]. No further investigations have been put into this area, it has been assumed that there is enough cooling available on-site or from the ocean. However, the purity of the water entering the PEM is of high importance and, if not pure enough, will influence both the hydrogen quality and technical lifetime of the electrolyzer [54]. Furthermore, the authors acknowledge that, given the production volumes of water, it is likely that the electrolyzer would require a dedicated water treatment plant (see Figure 2.1), incorporating ultra-filtration and reverse osmosis, to achieve the necessary water purity levels for the PEM.

2.6 Energy Storage Options as Flexibility Measures

To overcome the difficulties of having a variable energy source as input for e-fuel production, energy storage of different kinds can be deployed. The sizing of the energy storages is crucial to be able to operate the methanol synthesis, when there is a lack of wind. Wind variability can influence production on a daily, weekly, seasonal, and yearly level due to the characteristics of wind. For this work, hydrogen storage of two types (tank or rock caverns) and one type of Battery Energy Storage (BES), lithium-ion batteries, are considered.

2.6.1 Hydrogen Storage

Hydrogen can be stored physically, chemically, or through adsorption [55]. This case study has looked into the storage of hydrogen in pure, molecular form, that is, either in gas or liquid form (physical storage). Storing it physically is the most mature storage technology for hydrogen [56]. It can either be stored above or below ground, where the investments for aboveground storage solutions are noticeably higher for large-scale applications [55]. The large-scale applications of storing hydrogen below ground have been proven in the UK and the US [57]. However, this is for storage in

salt caverns, which is not something to consider, since suitable geological structures do not exist in Sweden.

The potential large-scale underground storage option in Sweden is the LRC, which has successfully been built in northern Sweden in pilot scale for the electrification of the steel industry [58]. The maximum size of the LRC has been determined using Hybrit's planned large-scale storage of maximum 65 GWh at an operating pressure of 250 bar. The LRC is excavated, forming a cylindrical vertical cavern in hard rock formations and is sealed with steel lining and a concrete outer layer to ensure a secure storage chamber [59]. Cushion gas of 10 % is needed in the chamber to sustain the minimum allowable pressure level, which influences the stability of the chamber [60].The technology has been proven successfully by construction and demonstration of a natural gas LRC facility called *Skallen*, located in southern Sweden [61].

Utilizing LRC as gaseous H_2 storage is related to frequent charging and withdrawal cycles, which causes pressure variations of the H_2 and determines the potential storage and withdrawal rates [62]. There are as of today lack in experience of LRC H_2 storages, which results in significant uncertainties when it comes to investment costs as well as the risk of hydrogen embrittlement of the steel lining, thus degrading the material drastically [62]. Currently, the most plausible storage technology is tanks [63]. Therefore, tanks have also been considered as a storage option, even though it is not practicable and economically feasible on a large scale [60]. Another reason for considering tank storage is the potential higher storing and withdrawal rates [64]. This is to ensure that if the hydrogen demand for the methanol synthesis exceeds the amount of hydrogen that can be withdrawn from the LRC, investments in additional tanks can solve that scenario. It has been assumed that H_2 tanks only have space limitations; other technical data has been retrieved from the Danish Energy Agency [64]. Storage of hydrogen usually requires high-pressure tanks with a tank pressure range of 350-700 bar. In this thesis, data for 200 bar tanks have been obtained from the Danish Energy Agency, since no collected data source was found for higher pressure levels. Due to the extremely low temperatures required for liquid storage of H_2 (below -250 ^oC), it has not been considered.

2.6.2 Batteries

Batteries have been considered as one of the energy storage solutions. The purpose of including a BES is to handle the wind variation to ensure that the methanol production can operate at all times according to technical requirements, such as minimum load level, ramp down, and ramp up rates. All system processes receive electricity supply either directly by the wind farm or through the battery. The battery will charge when there is an overproduction of wind power. For this case study, Lithium-ion batteries have been chosen due to several factors. Lithium-ion batteries offer the highest power and energy density compared to currently available alternatives [65]. For this kind of large-scale application, Lithium-ion batteries are the most mature and frequently used [66]. The high efficiency and fast charge/discharge rates of Lithium-ion batteries are also properties that outperform other options [65].

2.6.3 CO_2 Storage

CO_2 will be captured and supplied continuously through the already existing SMR in the Lysekil refinery. However, the methanol production rate might not align with the amount of CO_2 that is captured from the SMR process on site, thus CO_2 interim storage is necessary since the methanol production is expected to be influenced by varying hydrogen production from the wind farm. As of today, the CO_2 buffering technologies are not widely implemented, as the primary purpose of CO_2 transport to date has been utilization rather than storage [67]. Additionally, the ongoing CO_2 projects follow relatively simple supply chains, with few sources and a single sink, thus reducing the need for temporary storage. For this project, it has been assumed to utilize onshore steel storage tanks, since they are at a high Technology Readiness Level (TRL) and also well-suited for quayside buffers [67]. Alternatives, such as importing CO_2 from the Gothenburg refinery or exporting it for permanent storage, could be considered instead of using the CO_2 for synthesis. It is crucial to locate interim storage facilities close to the capturing site to minimize CO_2 transport distance and cost [67]. The buffer vessels are assumed steel alloy that fulfills the pressure and temperature requirements for the liquefied CO_2. For simplicity, cylindrical steel tanks have been considered, based on values and assumptions from the temporary storage site of Northern Lights [68]. While spherical tanks could also be feasible, they have not been explored in this study. Cooling requirement for the liquefied CO_2 has not been examined and is assumed to be included in the OPEX.

3
Methods

In this chapter, we present the methodology used to evaluate the feasibility of methanol production using offshore wind power, incorporated flexibility measures, and economic parameters. The methodology workflow described is illustrated in Figure 3.1.

Our approach integrates multiple analytical techniques, including a literature review to gather techno-economic data, process simulation of methanol synthesis in Aspen Plus, and a linear optimization model of the overall supply chain to minimize costs using the optimization tool GAMS. A methanol synthesis model was developed based on existing literature data, with parameters adjusted to optimize the conversion rate of reactants. The Aspen Plus model then supplied the greenfield investment model with process energy requirements and chemical reaction data. The cost minimization model is applied to a case study of the Preem Lysekil refinery, in section 3.5.

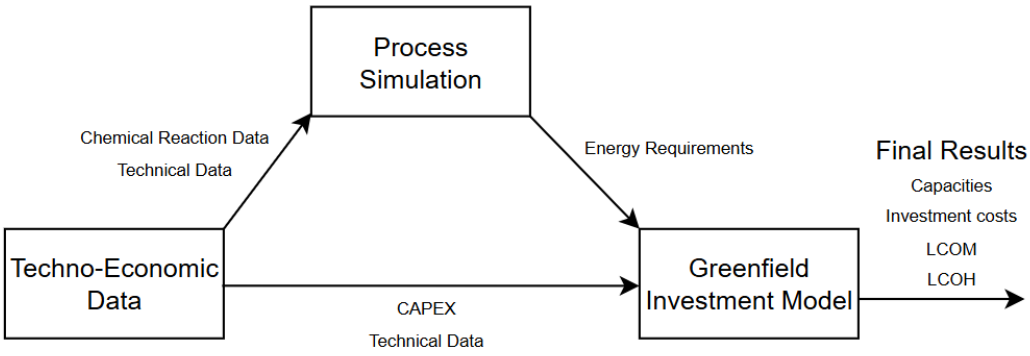

Figure 3.1: Illustration of methodology approach.

The Aspen Plus model will be presented in section 3.1 followed by the linear optimization model presented in section 3.3.

3.1 Methanol Synthesis Process Modeling

The process simulation for the synthesis of methanol was developed in Aspen Plus. While the flowsheet design seen in Figure 3.2 below is an original creation, it was conceptually inspired by previous studies focused on optimizing methanol production through direct CO_2 hydrogenation [69, 70].

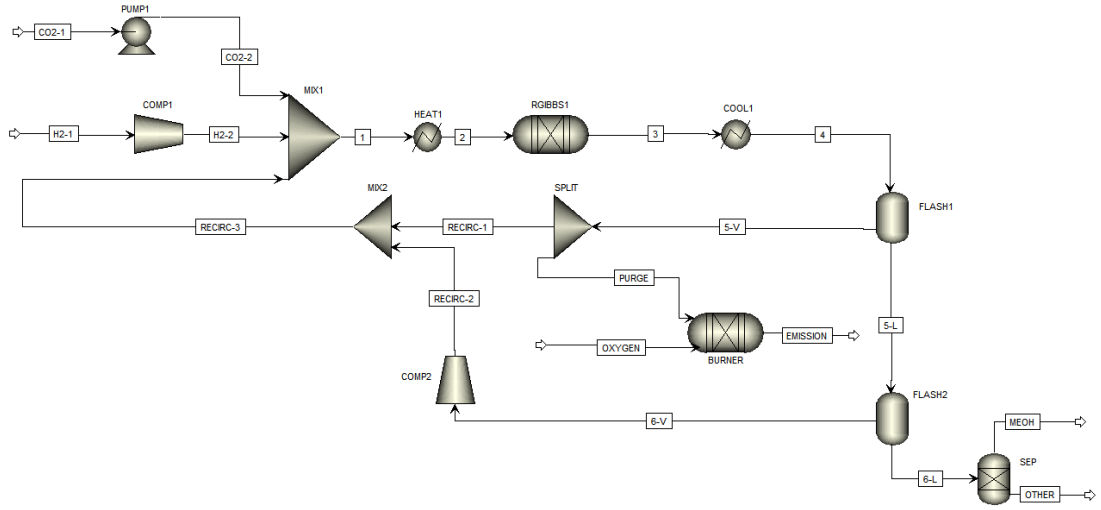

Figure 3.2: Methanol Synthesis flowsheet created in Aspen Plus.

These references guided key design considerations, such as the selection of the Soave-Redlich-Kwong (SRK) Equation of State as an appropriate thermodynamic model for simulating the methanol synthesis process.

Simulating thermodynamic equilibrium corresponds to an idealized case with infinite reaction residence time, which always allows the system to reach equilibrium regardless of reaction rates. While this simplifies the modeling process, it might not necessarily mirror reality, since in practice, kinetics may prevent the system from fully reaching equilibrium in an actual industrial process. However, this approach is still justified for the purposes of this thermodynamic analysis, since reaction kinetics were not considered in the project. Furthermore, the components considered in the simulation are limited to the products and reactants mentioned in 2.1 - 2.3, with the exception of O_2, only added to a separate reactor discussed later.

The flowsheet begins with the pure feed streams of hydrogen gas and carbon dioxide. It is assumed that pure H_2 gas is delivered from the electrolyzer at 80^oC and 30 bar, and fed to a compressor to be pressurized to the desired reaction pressure. On the other hand, the pure CO_2 feed is assumed to be delivered from a cryogenic separating unit, at -30 ^oC and 15 bar. Since the CO_2 is in liquid form, a pump is utilized to pressurize [71].

The feed streams are mixed with recycled unreacted reactants, and heated in a heater block set to the desired reaction temperature, before entering the reactor. Since the methanol synthesis reaction is exothermic and requires continuous cooling, an isothermal reactor was modeled using a RGIBBS block in Aspen Plus, considering both phase and chemical equilibrium, and calculating the product stream composition through on Gibbs Free Energy Minimization Method. The calculation method thermodynamically determines the most probable products under specified reaction conditions, and as such does not require defined kinetic or reaction stoichiometry parameters [72].

The reaction conditions were set to 220^oC and 80 bar. Following the reactor, product separation is modeled using a two-step flash process. Ahead of the first flash unit, the reactor output is cooled to 20^oC using a cooler to condense the products. At this stage, the vapor phase primarily consists of unreacted gases, is therefore separated in a flash unit and recycled back to the reactor. The condensed liquid phase, which still contains unreacted reactants, is sent to a second flash unit where it is depressurized to 1 bar. Again, the vapor stream is mainly reactants, and therefore recycled. However, before being mixed with the high pressure recycling stream, re-pressurization back to 80 bar by a second compressor. Notably, the vapor phase from the first flash unit is purged to avoid buildup of products in the recycling loop when Aspen iterates through the mass balances to find a steady state. Only 6% of the stream is separated into a purge stream, and is fed to a second Gibbs reactor along with a pure oxygen stream, simulating a burner to acquire some emission data.

Due to limitations in available data and the scope of the project, the detailed modeling of the purification was omitted. The remaining liquid, composed largely of products (methanol and water), was instead sent to a simplified separation, using a component separator block, which allowed for an exact splitting of methanol from water and negligible amounts of remaining reactants. The approach was deemed sufficient for the system-level analysis, where the exact column design and separation efficiency were not critical to the overall findings.

The flowsheet was completed with the selection of an appropriate inlet stream, in this case roughly 68,49 tonne CO_2 per hour (1556 kmol/h), equivalent to the total 600 000 tonnes per annum divided equally among the years hours. The resulting flowsheet is shown in Figure 3.2 below, which after simulation would yield the sought after results, including electricity consumption, carbon conversion and emission levels.

The conversion is calculated by comparing the incoming carbon feedstock *CO2-1*, as well as the outgoing *MEOH* streams. Using chemical calculations using mole masses of the different compounds, one can calculate the molar carbon conversion. On the same note, it can be concluded that the remaining carbon will leave the system either as CO_2 in *EMISSION* after combustion, or through some remaining CO_2 levels in the *OTHER* stream, and as such can be quantified as the inverse of the conversion.

While the model calculates both heating and cooling demands, these have been excluded from the energy balance calculations in the project. This is justified by the assumption that, in practice, such thermal requirements would be met by external utilities (i.e steam, seawater) rather than electricity. Additionally, the conceptual Aspen model does not incorporate heat exchangers between the streams, or the generating of steam from the continuous cooling of the reactor, something that would undoubtedly be executed in practice, to reduce utility demands. Consequently, the analysis focuses solely on electricity consumption associated with compression and pumping processes. To feed the data to the GAMS model as a parameter value, the

data is scaled to the mass unit of t/h.

3.2 Estimation of Compression Work

To accurately model the cost of utilizing storage technologies, it is important to consider variable costs, which in this case are the electricity required for compression, pumping and operation. In this study, the primary variable cost of storages is the electricity consumption for compressing hydrogen in the respective storage systems. As such, the electricity required for pumping liquid CO_2 into storage, as well as the variable operational costs associated with BES, were assessed to be negligible in comparison and therefore disregarded in model calculations.

3.2.1 Hydrogen Compression

The mechanical compression work of the compressor can be described by the following equations [73]. The resulting work, W [MWh/MWh_{H2}], is notably dependent on the initial temperature and desired pressure ratio, which are described in the case study 3.5. The parameter values used, as well as the results from the compression calculation, can be found in Table A.1 in the Appendix.

Equation 3.1 describes the isentropic post-compression temperature, T_2 [K], based on the pressure increase and the specific heat capacity ratio of the flow (k_{H2}).

$$T_{2s} = T_1 \left(\frac{p_2}{p_1} \right)^{\frac{k-1}{k}} \tag{3.1}$$

Next, Equation 3.2 is used to account for the isentropic efficiency of the compressor and determine the actual temperature at the outlet.

$$T_2 = T_1 + \frac{T_{2s} - T_1}{\eta_{is}} \tag{3.2}$$

The specific work, w [kJ/kg], of the gas undergoing compression can now be expressed by the difference in enthalpies, or by using the specific heat capacity and temperature difference, as seen in Equation 3.3 below.

$$w = h_2 - h_1 = C_p \times \Delta T_{2-1} \tag{3.3}$$

Lastly, the energy work is calculated by converting the energy unit and applying the lower heating value of hydrogen, LHV_{H2} [MWh_{H2}/kg_{H2}].

$$W = w \times \frac{1}{3600000} \times E^{-1} \tag{3.4}$$

3.3 Linear Optimization Model

The objective of the optimization model is to minimize the cost of an e-methanol production system on an annual basis using an hourly based time series. This is

achieved by finding optimal sizing and operation of process units, given boundary conditions such as wind power production profile, electricity price for SE3 and CO_2 feedstock profile. The linear optimization model was formulated and implemented in GAMS, with the cost-minimized system presented in section 2.4.

The sets, variables, and parameters used in the linear optimization model are summarized throughout Tables 3.1 -3.4. Table 3.1 defines the notation for all sets and variables, while Tables 3.2 and 3.3 present the parameter values related to storage and production technologies, respectively. The remaining model parameters are listed in Table 3.4. Both the notation and numerical values shown in these tables are consistently used throughout the explanation of the optimization model and its constraints in the following section 3.3.2.

Table 3.1: Description of sets and variables used in GAMS modeling.

Sets	**Description**	
T	Set of Time steps	$\{1, \ldots, 8760\}$
P	Set of Production technologies	{MeOH, PEM, WTP}
S	Set of Storage technologies	{H_2 Tank, H_2 LRC, Battery, CO_2, MeOH}
Variables	**Description**	
C_p	Annual Cost for Production technology P	[€]
C_s	Annual Cost for Storage technology S	[€]
C^{El}	Annual Cost of Electricity	[€]
C^{Em}	Annual Cost of Emission Tax	[€]
C^{Water}	Annual Cost of Water	[€]
$SOC_{S,t}$	State of Charge of Storage technology S at time step t	[MWh]
$Charge_{S,t}$	Charging of Storage technology S at time step t	[MWh/h]
$Discharge_{S,t}$	Discharging of Storage technology S at time step t	[MWh/h]
MtJ	Constant flow from MeOH storage to MtJ plant	[t/h]
$g_{P,t}$	Generation of Production technology P at time step t	[t/h, MWh/h, m^3/h]
Cap_S	Installed Capacity of Storage technology S	[MWh]
Cap_P	Installed Capacity of Production technology P	[t/h, MWh/h, m^3/h]
$El_{S,t}$	Electricity Demand for Storage technology S at time step t	[MWh/h]
$El_{P,t}$	Electricity Demand for Production technology P at time step t	[MWh/h]
$CO_{2_t}^{Input}$	Processed CO_2 in the MeOH Synthesis at time step t	[t/h]
$H_{2_t}^{Input}$	Processed H_2 in the MeOH Synthesis at time step t	[t/h]
$CO_{2_t}^{MeOH}$	CO_2 Transferred to MeOH Synthesis from CO_2 Feed at time step t	[t/h]
$H_{2_t}^{MeOH}$	H_2 Transferred to MeOH Synthesis from PEM at time step t	[t/h]
EL_t^{Max}	Wind Farm Maximum output at time step t	[MWh/h]
EL_t^{WF}	Purchased Electricity from Wind Farm at time step t	[MWh/h]
EL_t^{Grid}	Purchased Electricity from Grid at time step t	[MWh/h]
Em_t	CO_2 Emissions from MeOH Synthesis at time step t	[t/h]
Em^{Tot}	Total Emissions from system	[tCO2]
Em^{RFNBO}	Summarized CO_2 Emissions per tonne RFNBO	[tCO2/tRFNBO]

Table 3.2: Description of technical properties for storage technologies, used as parameters in GAMS modeling.

H_2 Tank				
c	Capital Expenditures	61000	[€/MWh]	[64]
OV	Operating Expenditures (Variable)	0.0409	[MWh/MWh_{H2}]	[Aspen Plus]
OF	Operating Expenditures (Fixed)	5	[% of CAPEX/year]	[Assumption]
η^C	Charging Efficiency	88	[%]	[64]
η^C	Discharging Efficiency	100	[%]	[64]
$Rate^C$	Charging Rate	0.6	[%/h]	[64]
$Rate^D$	Discharging Rate	100	[%/h]	[64]
N	Number of full charges and discharges	1000	[-]	[Assumption]
TL	Technical Lifetime	25	[years]	[64]
H_2 LRC				
c	Capital Expenditures	3190	[€/MWh]	[64]
OV	Operating Expenditures (Variable)	0.0474	[MWh/MWh_{H2}]	[Aspen Plus]
OF	Operating Expenditures (Fixed)	5	[% of CAPEX/year]	[Assumption]
η^C	Charging Efficiency	99	[%]	[64]
η^C	Discharging Efficiency	100	[%]	[64]
$Rate^C$	Charging Rate	0.21	[%/h]	[61]
$Rate^D$	Discharging Rate	0.42	[%/h]	[61]
N	Number of full charges and discharges	400	[-]	[61]
TL	Technical Lifetime	30	[years]	[61]
Battery				
c	Capital Expenditures	660000	[€/MWh]	[64]
OV	Operating Expenditures (Variable)	0	[€/MW]	[Assumption]
OF	Operating Expenditures (Fixed)	5	[% of CAPEX/year]	[Assumption]
η^C	Charging Efficiency	98.5	[%]	[64]
η^C	Discharging Efficiency	97.5	[%]	[64]
$Rate^C$	Charging Rate	50	[%/h]	[64]
$Rate^D$	Discharging Rate	100	[%/h]	[64]
N	Number of full charges and discharges	30000	[-]	[64]
TL	Technical Lifetime	25	[years]	[64]
CO_2				
c	Capital Expenditures	2000	[€/t]	[74]
OV	Operating Expenditures (Variable)	0	[€/t]	[Assumption]
OF	Operating Expenditures (Fixed)	5	[% of CAPEX/year]	[Assumption]
η^C	Charging Efficiency	30	[%]	[Assumption]
η^C	Discharging Efficiency	30	[%/h]	[Assumption]
$Rate^C$	Charging Rate	30	[%/h]	[Assumption]
$Rate^D$	Discharging Rate	30	[years]	[Assumption]
N	Number of full charges and discharges	1000	[-]	[Assumption]
TL	Technical Lifetime	30	[years]	[Assumption]
MeOH				
c	Capital Expenditures	300	[€/m^3]	[75]
OV	Operating Expenditures (Variable)	0	[€/MWh]	[Assumption]
OF	Operating Expenditures (Fixed)	5	[% of CAPEX/year]	[Assumption]
η^C	Charging Efficiency	100	[%]	[Assumption]
η^C	Discharging Efficiency	100	[%]	[Assumption]
$Rate^C$	Charging Rate	100	[%/h]	[Assumption]
$Rate^D$	Discharging Rate	100	[%/h]	[Assumption]
N	Number of full charges and discharges	-	[-]	[Assumption]
TL	Technical Lifetime	30	[years]	[Assumption]

Table 3.3: Description of technical properties for generating technologies, used as parameters in GAMS modeling.

Methanol Synthesis (MeOH)				
c	Capital Expenditures	7.465	[M€h/ton]	[64]
OV	Operating Expenditures (Variable)	5.68	[t/MWh]	[Aspen Plus]
OF	Operating Expenditures (Fixed)	5	[% of CAPEX/year]	[Assumption]
m	Minimum Load Level	30	[%]	[76],[77]
Rampdown	Operational Rampdown Rate	30	[%/h]	[76],[77]
Rampup	Operational Rampup Rate	30	[%/h]	[76],[77]
TL	Technical Lifetime	30	[years]	[64]
Electrolyzer (PEM)				
c	Capital Expenditures	2000	[€/KW]	[64]
OV	Operating Expenditures (Variable)	0.54	[MWhH_2/MWh]	[64]
OF	Operating Expenditures (Fixed)	5	[% of CAPEX/year]	[Assumption]
m	Minimum Load Level	0	[%]	[52]
Rampdown	Operational Rampdown Rate	100	[%/h]	[52]
Rampup	Operational Rampup Rate	100	[%/h]	[52]
TL	Technical Lifetime	25	[years]	[64]
Water Treatment Plant (WTP)				
c	Capital Expenditures	88115	[€/m^3]	[78]
OV	Operating Expenditures (Variable)	50	[MWh/m^3]	[78]
OF	Operating Expenditures (Fixed)	5	[% of CAPEX/year]	[Assumption]
m	Minimum Load Level	0	[%]	[Assumption]
Rampdown	Operational Rampdown Rate	100	[%/h]	[Assumption]
Rampup	Operational Rampup Rate	100	[%/h]	[Assumption]
TL	Technical Lifetime	25	[years]	[Assumption]

Table 3.4: Additional parameters used in GAMS modeling.

Parameters	**Description**	**Value**	**Unit**	**Source**
Cap^{WF}	Wind Farm Capacity	1225	[MW]	[Assumption]
Cap^{Grid}	Transmission Line Capacity from the Grid	100	[MW]	[Assumption]
WP_t	Normalized Wind Profile at time step t	-	[-]	[79]
$\text{CO2}_t^{\text{Feed}}$	Incoming CO_2 stream from SMR at time step t	-	[t/h]	[Preem]
LHV^{MeOH}	Lower Heating Value of Methanol	5.53	[MWh/t]	[64]
LHV^{H2}	Lower Heating Value of H_2	33.3	[MWh/t]	[64]
e^{SE3}	Emission Factor for Electricity Mix in SE3	2.44	[kgCO2eq/MWh]	[80]
e^{Limit}	Emission Limit to comply with RFNBO Regulations	0.1	[tCO2-eq/MWh]	[10]
η^{MeOH}	Molar Conversion Factor for MeOH Synthesis	92	[%]	[Aspen]
α^{H_2}	Reactions Stoichiometric Molar Mass Ratio CO_2:H_2	7.277	[t_{CO_2}/t_{H_2}]	[81]
α^{CO_2}	Reactions Stoichiometric Molar Mass Ratio MeOH:CO_2	0.728	[t_{MeOH}/t_{CO_2}]	[81]
Water^{Demand}	Water required for Electrolysis	0.178	[$m^3/MWh_{el,PEM}$]	[64]
C^{Water}	Cost of Unpurified Water	0.5	[€/m^3]	[Assumption]
C^{CC}	Cost of Carbon Capture	165	[€/t]	[Assumption]
C_t^{Spot}	Electricity Spotprice in SE3 at time step t	-	[€/MWh]	[82]
$\text{C}^{Energytax}$	Energy tax on purchased electricity from grid	50	[€/MWh]	[Assumption]
$\text{C}^{Gridfee}$	Transmission fee from purchasing electricity from grid	30	[€/MWh]	[Assumption]
C^{PPA}	Electricity Cost of PPA	70	[€/MWh]	[83]
C^{Em}	Cost of CO_2 Emissions Tax	134	[€/t]	[84]
r	Discount Rate	10	[%]	[85]
CRF_p	Capital Recovery Factor of Plant Technology p	-	[-]	[-]
CRF_s	Capital Recovery Factor of Storage Technology s	-	[-]	[-]

3.3.1 Objective Function

The objective function was formulated to minimize the total system cost, where both investment and operational costs were included. This means that the linear optimization decides which technology to invest in, at what capacity, how to operate each respective technology, as well as when and where to purchase the electricity, in order to minimize the total system cost. The objective function is presented in Equation 3.5 below.

$$\min \text{ Total Cost} = \sum_{p \in P} Cost_p + \sum_{s \in S} Cost_s + Cost^{Em} + Cost^{El} + Cost^{feedstock} \tag{3.5}$$

The annual fixed costs, $Cost_p$ and $Cost_s$, for production and storage technologies are calculated respectively accordingly.

$$Cost_p = CRF_p \cdot Cap_p \cdot c_p \cdot (1 + OF_p), \qquad \forall p \in P \tag{3.6}$$

$$Cost_s = CRF_s \cdot Cap_s \cdot c_s \cdot (1 + OF_s), \qquad \forall s \in S \tag{3.7}$$

The Capital Recovery Factor (CRF), used in the Equations 3.6 and 3.7, were calculated using the formula seen in 3.8, incorporating the discount rate and technical lifetime of the storage or plant technology.

$$CRF = \frac{r}{1 - (1 + r)^{-TL}} \tag{3.8}$$

The annual emission cost, $Cost^{Em}$, was calculated by adding up the varying hourly emissions from the process Em_t, over all time steps in T and multiplying the result by the Swedish carbon tax, as shown in Equation 3.9.

$$Cost^{Em} = C^{Em} \cdot \sum_{t \in T} Em_t \tag{3.9}$$

$Cost^{El}$, included in the objective function and described in Equation 3.10 below, is the total annual cost of electricity. The term accounts for both electricity purchased directly from the wind farm as well as from the grid, with the C^{PPA} price including all relevant fees or taxes.

$$Cost^{El} = \sum_{t \in T} \Big(El_t^{WF} \cdot C^{PPA} + El_t^{Grid} \cdot (C_t^{Spot} + C^{Energytax} + C^{Gridfee}) \Big) \tag{3.10}$$

The final cost variable included in the objective function accounts for the feedstocks required to operate the electrolyzer (water) and the methanol synthesis unit (captured CO_2), in addition to the electricity already sourced via the grid or the PPA. The total annual cost of these feedstocks, shown in Equation 3.11, is linearly proportional to the quantities of purified water and utilized CO_2.

$$Cost^{feedstock} = C^{Water} \cdot \sum_{t \in T} g_{WTP,t} + C^{CC} \cdot \sum_{t \in T} CO2_t^{\text{Feed}} \cdot C^{CC} \tag{3.11}$$

3.3.2 Model Constraints

This section outlines the key mathematical constraints implemented in the model. It is structured into four parts: constraints on production technologies, storage dynamics, electricity flows and balances, and lastly emissions. Each group of constraints reflects the technical, operational, and policy related limitations that govern the modeled energy system.

3.3.2.1 Technology Constraints

The hourly generation of each production unit cannot exceed the installed capacity, as seen in Equation 3.12.

$$Cap_p \geq g_{p,t} \qquad \forall p \in P, \forall t \in T \tag{3.12}$$

The practical and technical limitations of the plant technologies outlined in Chapter 2 and detailed in Table 3.3 were implemented into the model. These begin with ramp-up/down rates, which constrain how quickly production can change relative to installed capacity, seen in Equations 3.13 and 3.14. The last constraint, displayed in 3.15, define the hourly production rates cannot go below the minimum load, applicable to the synthesis and electrolysis.

$$Cap_p \cdot Rampup_p \geq g_{p,t+1} - g_{p,t} \qquad \forall p \in P, \forall t \in T \tag{3.13}$$

$$Cap_p \cdot Rampdown_p \geq g_{p,t-1} - g_{p,t} \qquad \forall p \in P, \forall t \in T \tag{3.14}$$

$$Cap_p \cdot m_p \leq g_{p,t} \qquad \forall p \in P, \forall t \in T \tag{3.15}$$

The energy and mass balances were individually set for each plant technology. For the electrolyzer, the generated H_2 was defined through an energy balance that defines the different paths it could take. Equation 3.16 states that all the produced H_2 must be equal to the amount charged in the storages and the amount transferred directly to the synthesis of methanol at each time step t.

$$g_{PEM,t} = Charge_{LRC,t} + Charge_{Tank,t} + H2_t^{MeOH} \qquad \forall t \in T \tag{3.16}$$

For the methanol synthesis, a mass balance was used to ensure that the amount of methanol produced was limited by the reactions stoichiometry and conversion efficiency. As such, the mass produced methanol was calculated as the mass processed CO_2, multiplied by the conversion factor estimated from the Aspen simulations. To account for the difference in molecular weight between the two compounds, the ratio between molar masses was incorporated into the calculation. This relationship is expressed in Equation 3.17.

$$g_{MeOH,t} = CO2_t^{Input} \cdot \alpha^{CO_2} \cdot \eta^{MeOH} \qquad \forall t \in T \tag{3.17}$$

In addition to CO_2, the reaction also requires H_2. To ensure the model reflects the correctly balanced consumption of reactants, Equation 3.18 was added as a constraint. The formula defines the amount of respective processed reactants ($H2_t^{Input}$, $CO2_t^{Input}$) by accounting for stoichiometry and unit conversions.

$$CO2_t^{Input} = \frac{H2_t^{Input}}{LHV^{H_2}} \cdot \alpha^{H_2} \qquad \forall t \in T \tag{3.18}$$

While the CO_2 storages mass balance will be defined trough the broader Equation 3.22, the mixing point around the CO_2 feedstock, storage and methanol plant inlet needs to be designated separately. This was incorporated through the implementation of Equations 3.19 and 3.20.

$$CO2_t^{Feed} = CO2_t^{MeOH} + Charge_{CO2,t} \qquad \forall t \in T \tag{3.19}$$

$$CO2_t^{Input} = CO2_t^{MeOH} + Discharge_{CO2,t} \qquad \forall t \in T \tag{3.20}$$

The hourly generation of the water treatment plant was defined to equate the hourly demand of purified water the electrolyzer required. This was deemed a reasonable simplification due to the assumption that both technologies were fully flexible within the hour, removing the need for an intermediate purified water storage, in the model. The water demand parameter specifies the volume of purified water required for every unit of electricity consumed by the electrolyzer, showcased in Equation 3.21.

$$g_{WTP,t} = El_{PEM,t} \cdot Water^{Demand} \qquad \forall t \in T \tag{3.21}$$

3.3.2.2 Storage Dynamics

The key constraint in storage dynamics is the storage balances, where the hourly stored quantity is referred to as *State of Charge* (SOC). Equation 3.22 shows how the level depends on the level of the previous time step, and is adjusted based on the storage that is charged or discharged during the time step.

$$SOC_{s,t} = SOC_{s,t-1} + Charge_{s,t} - Disharge_{s,t} \qquad \forall s \in S, \forall t \in T \tag{3.22}$$

Similar to the technology capacity's definition in Equation 3.12 , the storage capacity is defined as the highest SOC during the modeled period, as seen in Equation 3.23

$$Cap_s \geq SOC_{s,t} \qquad \forall s \in S, \forall t \in T \tag{3.23}$$

Additionally, constraints were implemented to account for the practical storage dynamic limits. Equation 3.24 and 3.25 charging and discharging to the maximum rate for the storage size, while Equation 3.26 limits how many times the storage can cycle per year, in order to prevent excessive lifetime degradation.

$$Charge_{s,t} \leq Rate_s^C \cdot Cap_s \qquad \forall s \in S, \forall t \in T \tag{3.24}$$

$$Discharge_{s,t} \leq Rate_s^D \cdot Cap_s \qquad \forall s \in S, \forall t \in T \tag{3.25}$$

$$\sum_{t \in T} Charge_{s,t} \leq \frac{Cap_s \cdot N_s}{TL_s} \qquad \forall s \in S \tag{3.26}$$

Notably, unlike the other storages, the methanol storage is not operated flexibly, seen in Equations 3.27 and 3.28. As one of the final steps, its charging is simply equal to the methanol synthesis plants generation, and its discharge is equal to the size of the flow to the MtJ plant, outside of the boundary. The feed is a constant variable, as its value would determine the size of the less flexible MtJ process.

$$Charge_{MeOH,t} = g_{MeOH,t} \qquad \forall t \in T \tag{3.27}$$

$$Discharge_{MeOH,t} = MtJ \qquad \forall t \in T \tag{3.28}$$

3.3.2.3 Electricity Balance

Defining electricity flows and balances begins with the sources, the offshore wind farm and the grid.

While the model and case study does not consider a limit on electricity purchased per annum, the hourly purchase E_t^{WF} will in practice be limited by the wind farms hourly production E_t^{Max}. Equation 3.29 accounts for the varying wind profile, while 3.30 sets the limit on how much electricity can be bought hourly from the wind farm. The power consumed through the grid is limited by the installed transmission capacity, as seen in Equation 3.31.

$$El_t^{max} = Cap^{WF} \cdot WP_t \qquad \forall t \in T \tag{3.29}$$

$$El_t^{WF} \leq El_t^{Max} \qquad \forall t \in T \tag{3.30}$$

$$El_t^{Grid} \leq Cap^{Grid} \qquad \forall t \in T \tag{3.31}$$

The electricity consumption for each production technology is defined using the technologies generation and its specific electricity consumption, as seen by equation 3.32. For this equation the variable OPEX OV had to be adapted to fit the equation since they were expressed in different units.

$$El_{p,t} = \frac{g_{p,t}}{OV_p} \qquad \forall p \in P, \forall t \in T \tag{3.32}$$

For the storage technologies N equation 3.33 was expressed to track the energy needed for pumping, compression, or other energy-intensive processes to keep each subsystem functioning.

$$El_{s,t} = Charge_{s,t} \cdot OV_s \qquad \forall s \in S, \forall t \in T \tag{3.33}$$

After defining both purchased and consumed electricity, the overall electricity balance for the system can be established. Since the utilization of the different units

is interdependent, the balance equation captures how they interact. Each term on the left side of Equation 3.34 represents electricity supplied to the system, while the right side includes all consuming terms.

$$El_t^{WF} + El_t^{Grid} + Discharge_{Battery,t} = \sum_{p \in P} El_{p,t} + \sum_{s \in S} El_{s,t} + Charge_{Battery,t} \qquad \forall t \in T \quad (3.34)$$

3.3.2.4 Emissions Calculations

Lastly, the models constraints is concluded with emission calculations.

Section 3.1 explains that the methanol synthesis plant does not yield full conversion of CO_2 into MeOH, and how the unreacted share is combusted in a burner. Equation 3.35 calculates the hourly varying emissions using the unreacted share of the processed CO_2.

$$Em_t = CO2_t^{\text{Input}} \cdot (1 - \eta^{\text{MeOH}}) \qquad \forall t \in T \quad (3.35)$$

The policy around RFNBO discussed in 2.3, require the fuel to reduce emissions by 70%, compared to fossil fuels. Therefore two emission constraint were implemented. Equation 3.36 defines Em^{Tot}, the collective carbon intensity from the RFNBOs production (process and grid emissions), calculated over the production year. The second constraint, Equation 3.37, limits Em^{Tot} to adhere to EU policy.

$$Em^{Tot} = \frac{\sum_{t \in T} \left(e^{SE3} \cdot El_t^{Grid} + Em_t \right)}{\sum_{t \in T} g_{MeOH,t}} \quad (3.36)$$

$$e^{Limit} \geq Em^{Tot} \quad (3.37)$$

3.4 Key Performance Indicators

In order to evaluate the objectives outlined in 1.1, certain *Key Performance Indicators* (KPIs) beyond the objective of the LP model are required to understand different parts of the supply chain. *Levelized Cost*, for different products in the system, was identified as the most useful and appropriate performance indicator for the study. The resulting value includes the infrastructure and operational costs required for the production, and is proportional to the quantity produced. Additionally, Levelized Cost is a useful metric to compare the production with other scenarios, such as changing of parameters or comparing with competing market prices. The report will consider the three KPIs listed below.

- **Levelized Cost of Hydrogen (LCOH)**:
  Expressed in the unit [€/kg H_2], LCOH represents the cost per unit of hydrogen produced by incorporating the total capital and operational costs solely related to its production. In this case, the electrolyzer and water plant investment, electricity and water inputs, and any relevant storage investments, as

seen in Equation 3.38.

- **Levelized Cost of Methanol (LCOM)**:
  As previously discussed, EU policy defines different tiers of fuels depending on ingoing feedstock and energy. Due to the utilization of grid power in some scenarios, it is essential to differentiate between the quantity of methanol produced, and the share that is actually e-MeOH (RFNBO). As such, LCOM [€/t MeOH] will be the metric that values the totality of produced methanol, and is calculated using the same reasoning as previously discussed, seen in Equation 3.39.

- **Levelized Cost of RFNBO Methanol ($\boldsymbol{LCOM_{\mathrm{RFNBO}}}$)**:
  Specifically refers to the levelized cost of methanol classified as RFNBO, as discussed in 2.3. Calculated in Equation 3.40, this KPI serves to isolate the economic viability of the RFNBO fraction of methanol production. Notably, the share of RFNBO methanol is quantified using the indicator X_{RFNBO} defined in Equation 3.41, where the share of renewables in SE3 (X_{SE3}) has been assumed to be 30 %.

$$LCOH = \frac{Cost_{PEM} + Cost_{WTP} + Cost_{H2Tank} + Cost_{H2LRC}}{\sum_{t \in T} g_{PEM,t}} \tag{3.38}$$

$$LCOM = \frac{\text{Total Cost}}{\sum_{t \in T} g_{MeOH,t}} \tag{3.39}$$

$$LCOM_{\mathrm{RFNBO}} = \frac{\text{Total Cost}}{\sum_{t \in T} g_{\mathrm{MeOH},t} \cdot X_{\mathrm{RFNBO}}} \tag{3.40}$$

$$X_{\mathrm{RFNBO}} = \frac{\sum_{t \in T} \left(EL_t^{\mathrm{WF}} + EL_t^{\mathrm{Grid}} \cdot X_{\mathrm{SE3}} \right)}{\sum_{t \in T} \left(EL_t^{\mathrm{WF}} + EL_t^{\mathrm{Grid}} \right)} \tag{3.41}$$

All the cost terms in the nominator in Equation 3.38 were calculated identically, as seen in Equation 3.42, where the subscript j embraces the units of interest, $J = \{\mathrm{PEM}, \mathrm{WTP}, \mathrm{H_2Tank}, \mathrm{H_2LRC}\}$. In all scenarios, a simplification was made regarding electricity cost calculations of LCOH. Instead of distinguishing between electricity bought from the power purchase agreement (C^{PPA}) and the spot price (C_t^{spot}) for each hour of operation, only C^{PPA} was used. This approximation does not affect the overall conclusions, as almost all electricity is supplied by the PPA, and the small amount drawn from the grid has a negligible effect on the results over a yearly basis.

$$Cost_j = C_j + C_j \cdot OF_j + C^{PPA} \cdot \sum_{t \in T} El_{j,t} \qquad \forall j \in J \tag{3.42}$$

To evaluate the long-term economic viability of the project, the study uses the *Net Present Value* (NPV) as an additional KPI. Unlike previously discussed indicators, NPV accounts for the time value of money across the entire project lifetime. As seen in Equation 3.43, the NPV at year T is computed as the sum of all discounted cash flows C_t, where t is the year index and r is the discount rate.

The technical lifetime of the units differs, but since 25 years is the lowest, it was also assumed to be the system's lifetime. However, T was set at 28, due to the first three years representing the construction period of the methanol plant, where cash flow was the negative investment cost equally divided between the three years. Starting from the first operational year (year 3), the plant is assumed to be running uninterrupted under constant conditions for the remaining years, with the cash flow being defined as the operational costs subtracted from the revenue (produced product multiplied by a fixed market price).

$$NPV = \sum_{t \in T} \frac{C_t}{(1+r)^t} \tag{3.43}$$

The utilization of the available wind energy from the Mareld offshore wind farm (UF_{Wf}) will also be calculated and is expressed in equation 3.44.

$$UF^{WF} = \frac{\sum\limits_{t \in T} El_t^{WF}}{\sum\limits_{t \in T} El_t^{Max}} \tag{3.44}$$

3.5 Case Study

The thesis has looked into the scenario of producing methanol utilizing CO_2 captured onsite, together with hydrogen produced using an electrolyzer powered by offshore wind. The CO_2 is captured from an already existing SMR process, where CO_2 is created as a byproduct when producing hydrogen, which is used for other fuels and processes on-site (see figure 3.3). The methanol will be one of the key components used to produce jet fuel through a MtJ process.

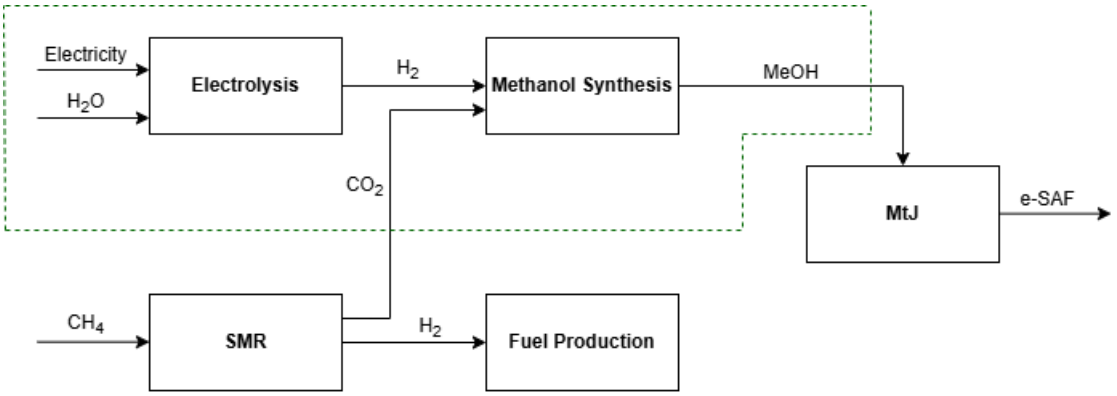

Figure 3.3: Simplified system boundary of the case study.

This work has assumed that the SMR has a cryogenic CO_2 capturing process because it can achieve almost 100 % CO_2 concentration, outperforming other technologies [86]. As a result, no further conditioning or purification is required before the CO_2 enters the methanol synthesis stage, which is a desirable feature since the $Cu/ZnO/Al_2O_3$ catalyst is highly sensitive to impurities, particularly sulfur [87], [88]. This sensitivity is one reason why more mature capture technologies, such as amine-based CO_2 capture, may be less suitable, aside from concerns regarding their toxicity. Another advantage of having a high purity level is that it not only reduces the risk of catalyst deactivation, but also minimizes the formation of unwanted, corrosive byproducts. The cryogenic capture also delivers CO_2 in liquid form, which is more dense than in gaseous form, enabling smaller storage systems, thus reducing material and energy costs [89]. The system model only includes a cost of 165 €/t for the cryogenic CO_2 capture, which is assumed to include both CAPEX and OPEX. Therefore, no additional energy requirements calculations have been performed. However, the emissions related to the cryogenic capturing process have not been taken into account. It is important to note that the excluded emissions from the capture process could influence the overall GHG emission results, particularly when evaluating compliance with the 70 % savings threshold required for RFNBO classification. Therefore, the CO_2 is only considered as an input stream from the SMR unit to the methanol synthesis with an associated cost included in the objective function (see figure 2.1). The production goal of e-methanol is set by the annual supply of 600 000 tonnes CO_2, which is the limiting factor for how much methanol can be produced during one year. In the model, the CO_2 stream is assumed to be supplied following an hourly profile similar to the production pattern of the current operating SMR unit at the Lysekil site, but scaled to correspond to 600 000 CO_2 t/a. The methanol storage will act as a buffer to be able to operate the less flexible MtJ process, since it does not allow rapid load changes in the production phase.

The offshore wind farm is assumed to align with the project Mareld, which Freja Offshore is responsible for and investigating. The location of the wind farm is estimated to be 30-40 km outside the coast of the Lysekil refinery. The government has not approved the wind farm as of today, but it is planned to consist of a total of 2450 MW installed capacity of floating wind turbines [90]. The proposed wind farm is planned to be located in a Natura 2000 area, which requires a special permit from the County Administrative Board of Västra Götaland. This permit was granted in March 2025, which means that the last step is to get an approval from the government. It is assumed that the wind farm will in reality consist of 165 identical floating wind turbines of the model Vestas V-236-15 MW, summing to a total capacity of 2450 MW. However, in this case it is assumed that Preem, or any other actor, will not have access to the full capacity of the wind farm. Instead, only half of the total capacity (1225 MW) is assumed to be available for Preem. This means that when the wind farm operates at 100% load, only 50% will be accessible, and at 10% load, only 5% would be available. The additional capacity (remaining 1225 MW) is assumed to be connected to the grid, which does not interfere with the RED prerequisites [44]. However, this is not considered in the model.

The maximum height of the turbines is restricted to 350 meters, and the wind data has been extracted using Mattsson's developed model (for more information, see Appendix B). This project only has considered data in the model adapted to 15 MW turbines, more specifically Vestas's model V-236-15 MW. No decline in performance during the wind farm lifetime has been assumed since the model only runs for 1 year, even though it will have an influence long-term.

The construction time of the wind farm has been estimated to be 4 years, according to Freja Offshore AB, and for this work, to fulfill the RFNBO, the wind farm is assumed to be established simultaneously as the fuel production plant. The refinery is assumed to have a PPA with Mareld, with the electricity price set to the levelized cost of offshore wind power, estimated at 70€/MWh [83]. This price will be varied in the sensitivity analysis to evaluate its impact on the production cost of methanol. The PPA is assumed to include all the associated costs. Additionally, no energy taxes or transmission fees are considered, as the electricity is supplied directly from the wind farm without utilizing the electricity grid. However, for the electricity price taken from the grid, an additional energy tax and transmission fee of 50 €/MWh and 30 €/MWh, respectively, are assumed to be added to the spot price. The spot price data was taken from Nord Pool´s database, and 2019 was used as a reference year. Additionally, it is assumed that the plant will be able to access grid electricity in the SE3 bidding zone, with the model being fed hourly spot prices (for the corresponding wind year). Onshore wind has not been investigated due to a lack of public acceptance and logistical reasons for installing a wind farm of Mareld's magnitude.

Since this case study evaluates the potential for cost-effective methanol production on the west coast of Sweden, comparing the methanol production costs that can be achieved with imported hydrogen is highly relevant. Given the significant variation in the Levelized Cost of Hydrogen (LCOH), scenarios involving the import of H_2 will be investigated to determine whether importing H_2 leads to a notable difference in the overall production costs of methanol. This study will not examine different types of LOHC for transport. Instead, it will focus on transport costs derived from previous studies, where the estimated cost of transporting liquefied hydrogen to Northern Europe is 1.5 €/kg H_2 if sourced from North Africa, 2.6 €/kg H_2 from Chile, and 3.7 €/kg H_2 from Australia (where liquefaction, transport and distribution costs are included in the cost value) [91].

It was assumed that the large amount of oxygen produced from the PEM will not be utilized on site or conditioned so that is can be exported. It is worth noting that a previous study at Lysekil refinery concluded that potential revenues from local oxygen export were limited, because of the large volumes [60].

3.6 Scenarios

This study will investigate five scenarios (see Table 3.5). The first one, called *Full Flex*, is the base case, where all possible flexibility measures related to H_2 produc-

tion (electricity and H_2 storage) can be invested in (see Table 3.5). However, no electricity can be taken from the grid, meaning that the system is self-sufficient with wind farm electricity. The reason for this is the base case is to investigate how the other flexibility measures, as well as the electricity grid, influence the investment costs and the RFNBO requirements. The second scenario, called *Full Flex Grid*, is similar to the first one, but there is a possibility to use electricity from the grid. The third case, named *Battery*, only includes a BES to handle variations in the system, but is also connected to the grid. The fourth scenario, H_2, is almost identical to the previous one, except that it consists of an H_2 storage system instead of a BES. Finally, the *No Flex* scenario will be considered, where no H_2 production flexibility measures are available, but there is unlimited supply from the grid. This is done to determine how much RFNBO is actually produced if one is fully allowed to use grid electricity.

All scenarios include CO_2 storage, as any CO_2 not used in the synthesis process or for another purpose will be temporarily stored before being shipped to permanent storage. The inclusion of MeOH storage in all scenarios is due to the fact that the produced fuel will be stored to some extent at the refinery. plus, required for operability of downstream processing units with lower flexibility.

All of the scenarios that have the grid transmission line available as an energy source are subject to a transmission limitation of 100 MW output, except for *No Flex*, which, as mentioned previously, is given unlimited transmission capacity. This is done to observe the share of RFNBO that is produced and also to enable comparison with the scenarios that include flexibility measures.

Table 3.5: Visualization of flexibility measures available in each scenario.

	Grid	**Battery**	**H_2 storage**	**CO_2 storage**	**MeOH storage**
Full Flex	-	✓	✓	✓	✓
Full Flex Grid	✓	✓	✓	✓	✓
Battery	✓	✓	-	✓	✓
H_2	✓	-	✓	✓	✓
No Flex	✓	-	-	✓	✓

4

Results

In this chapter, the results for all scenarios will be presented, followed by a sensitivity analysis of the cheapest system configuration (*Full Flex grid*), where the cost of PPA, wind data, CAPEX of electrolyzer, η_{PEM}, minimum load and ramp up/down rates of the methanol synthesis will be varied to see if the local methanol production can be cost-effective. The wind data will also be varied to see to how large extent it influences the results.

4.1 Aspen Modeling Results

After simulating the flowsheet in Figure 3.2, the results can be directly seen in the flowsheet, as seen in Figure 4.1 below, and through some calculations and unit conversions, laid out in 3.1, the sought after results are displayed in Table 4.1.

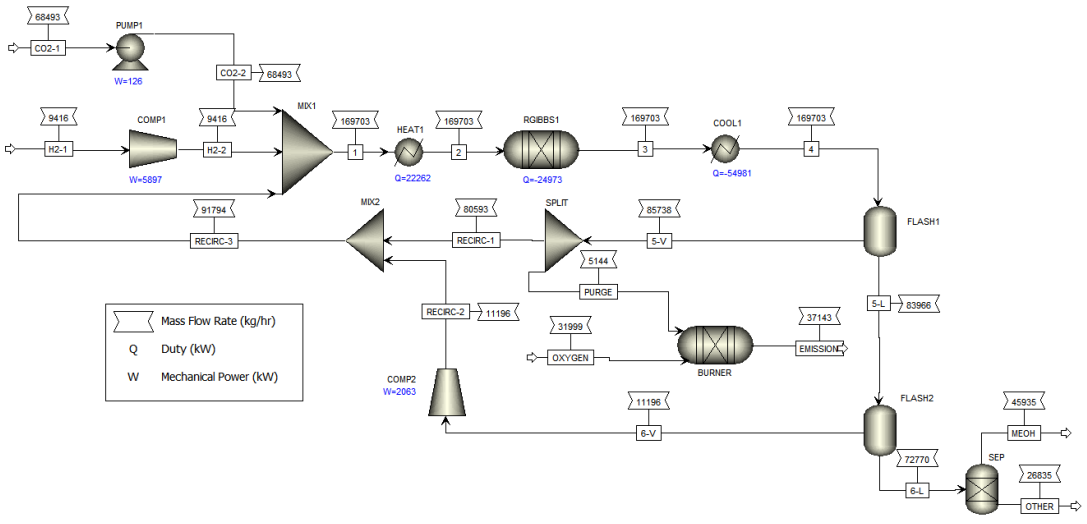

Figure 4.1: Results from Aspen simulation of methanol synthesis.

Table 4.1: Calculated and converted Aspen modeling results for GAMS modeling.

	Value	**Unit**
CO_2 Conversion	92	[%]
CO_2 Emission	8	[%]
Electricity Consumption	0.176	[kWh/t MeOH]

Reflecting on the results obtained, the conversion efficiency of 92%, is slightly lower than values seen achieved in the literature. For example, a study by Mbatha et al.(2024) investigated and modeled several different power-to-methanol process configurations in Aspen Plus and consistently achieved CO_2 conversions within the 98-100% range [92]. However, given that this flowsheet was only a conceptual design, lacking the more complex recycle loops and separation steps, the result is well within the expected range, and serves adequately as a basis for system-level modeling.

Additionally, it is noteworthy that the electricity consumption to prepare the reactant feed prior to synthesis is comparatively lower than other designs found in the literature. This is also partly due to the simplified model setup, but also due to the nature of the case study. Firstly, unlike most cases in literature, the CO_2 feed is obtained from a cryogenic capturing unit, and is already delivered somewhat pressurized and in liquid form. This approach reduces the overall energy demand for the compression, as liquid-phase pumping generally requires significantly less energy than compressing gases. Secondly, the hydrogen stream delivered from the PEM electrolyzer enters the synthesis loop at elevated pressure (30 bar assumed), further minimizing the additional compression work. These specific characteristics of the case study contribute to the low reported electricity consumption, which aligns with values presented in Concawe's techno-economic assessment of e-fuels [91].

Finally, it is important to note that the Aspen model assumes steady-state operation and does not capture deviations that occur during partial load operation or during ramping. While these dynamic effects are important in practice, in particular when integrating with intermittent renewable energy sources, they are compensated for in the broader system-level GAMS model through constraints on minimum load and ramp rates. In conclusion, the Aspen modeling was primarily used to verify a baseline for conversion and energy requirements, both of which proved adequately consistent with literature, enough for integration in the broader GAMS system-wide model.

4.2 Overview of Cost-Optimal System Results

The optimization model results in an energy system that balances the intermittency of wind with the sizing of key components. The model was feasible for the base case, *Full Flex*, a fully autonomous system, solely relying on energy from offshore

wind, with access to all flexibility measures except access to grid electricity. While serving as a benchmark against the other scenarios, it is also useful to provide a general understanding of how the optimized systems are configured, how energy flows through the supply chain, and what the resulting cost breakdowns look like. Table 4.2 showcases notable KPIs (LCOM excluded due to 100% RFNBO share), setting the stage for subsequent sections.

Table 4.2: Full Flex results.

	Value	**Unit**
RFNBO Produced	402	[kt/a]
Annual Cost	647	[M€/a]
$LCOM_{RFNBO}$	1612	[€/t]
LCOH	5.76	[€/kg]

The Sankey diagram in Figure 4.2 shows what the annual energy flows look like for *Full Flex*. The main energy flows for each scenario do not vary significantly. Approximately 5.2 TWh of wind energy is needed to produce 2.3 TWh of e-methanol, where the heat losses from the electrolysis are higher than the actual methanol output. The total energy demand corresponds to more than 55 % of the current electricity demand from the whole industry in Gothenburg [93]. The resulting power-to-methanol efficiency, converting electricity to methanol, is around 40 to 42 %. It can be concluded that the largest loss occurs in the electrolysis, which is why reaching a high H_2 production efficiency is highly relevant. This will be investigated further in the sensitivity analysis to see how much it influences the $LCOM_{RFNBO}$.

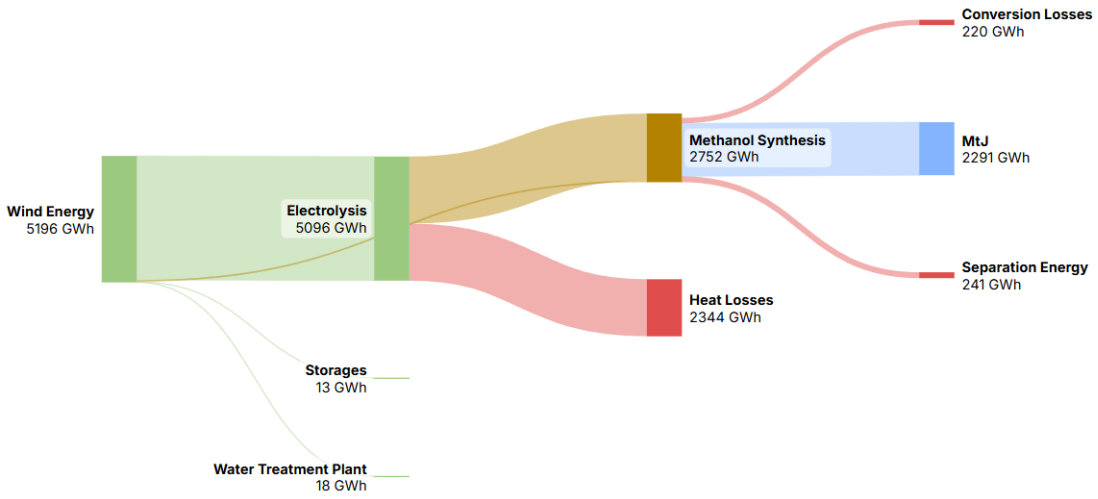

Figure 4.2: Sankey diagram of energy flows and losses in *Full Flex* scenario.

Figure 4.3 outlines how the annual cost is composed in the *Full Flex* system. The electricity procurement accounts for around half of the expenditure, with the invest-

ments in methanol synthesis, electrolyzer, and the cost of carbon capture accounting for the other notable segments. The flexibility measures (specifically the LRC and BES) incur a relatively small cost, but are nevertheless key to enable continuous methanol production in a non-grid configuration. This was then proven by the models' infeasibility, when the ability to purchase from the grid was removed.

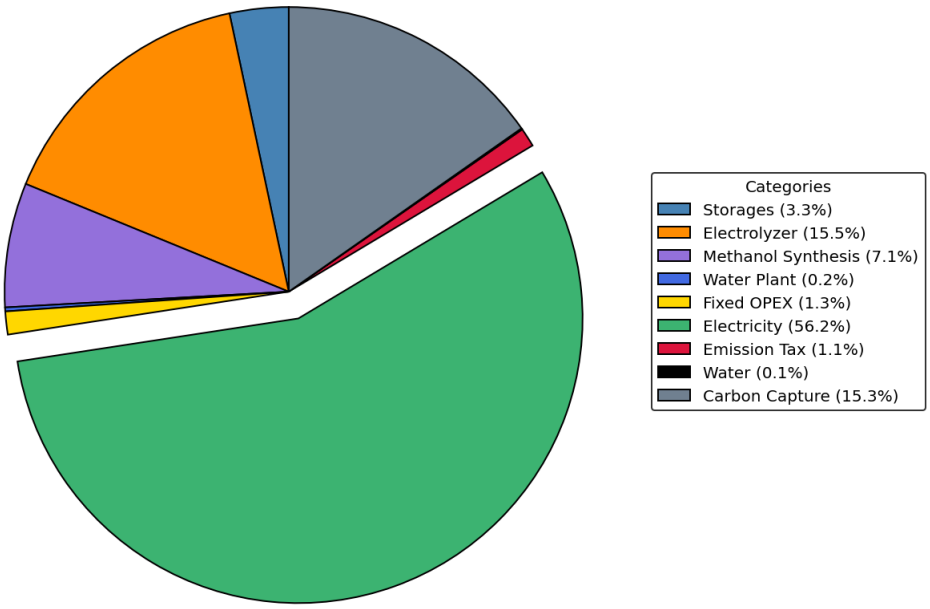

Figure 4.3: Resulting annual cost distribution of system in the *Full Flex* scenario.

4.3 Value of Flexibility Measures and Feasibility

Comparing the different scenarios shows to what degree the different flexibility measures provide value to the system and how they are essential for technically feasible operation.

One way to display how the operation was handled following the loss of key flexibility capabilities is by analyzing the scale of investments in key units. Table 4.3 indicates that the H_2 LRC provides the most cost-effective flexibility out of all the storages, and is invested in each scenario where it was available. The mathematical reasoning seemingly is that the LRC is notably cheaper than the BES, making it cheaper to produce excess hydrogen during high wind availability and storing it for less windy hours than it was to store the energy in batteries. Both of which would have enabled the stable operation of the minimum load constrained synthesis plant. Additionally, no optimized scenario selects the H_2 Tank, always opting for the LRC. Yet while the results demonstrate great potential, the geological feasibility of large-scale underground H_2 storage remains unexamined. Further investigation

is required to determine whether suitable geological formations exist at Lysekil refinery to support this technology.

Table 4.3: Overview of notable installed capacities of storage and technology units, in each scenario

Unit	**Full Flex**	**Full Flex grid**	**Battery**	**H_2**	**No flex**
PEM [MW]	455	428	368	428	383
MeOH [t/d]	1386	1383	1288	1383	1344
H_2 LRC [GWh]	28.2	15.8	-	15.8	-
H_2 Tanks [MWh]	0	0	-	0	-
BES [MWh]	52.3	0	3211	-	-

On the other hand, out of the three scenarios where BES was available, it was only selected in two, seemingly only opted for when either grid capacity or hydrogen storages were unavailable. Although they offer better the fastest flexibility, the high CAPEX makes them less attractive than other flexibility measures, even though they can reduce the oversizing of the costly electrolyzer, increasing its capacity factor. This can notably be observed in the *Battery* scenario. When the hydrogen storages are removed, leaving BES as the essential flexibility measure for feasibility, the PEM investment falls significantly, but an enormous investment in BES was required, as shown in Figure 4.4 . Furthermore, the only outlier in methanol synthesis capacity is found in the *Battery* scenario, which can be attributed to the same effect, where the model opts for a reduced capacity, in turn lowering the minimum load threshold, in a system where being flexible becomes very expensive.

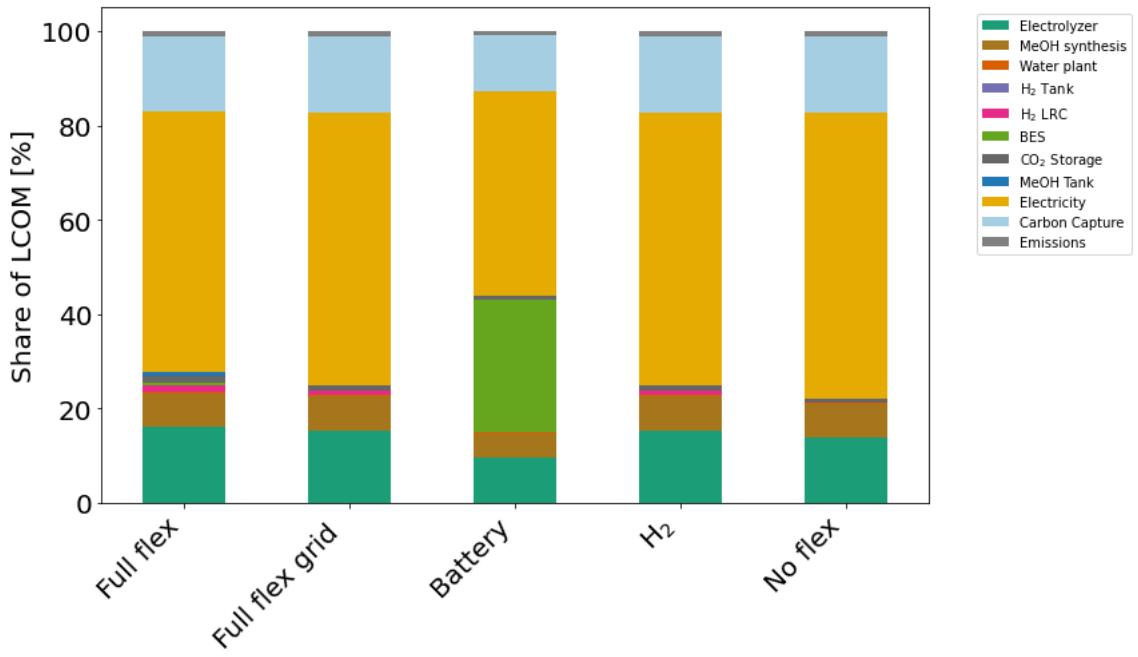

Figure 4.4: Cost distribution of resulting LCOM in each scenario.

Grid connection capability also adds considerable value in maintaining technical feasibility. In scenarios where BES or hydrogen storage was removed, the grid power acted as a balancing mechanism to meet the minimum load constraints of the methanol synthesis during windless hours. In fact, the model even proved infeasible for the *No Flex* and H_2 scenarios when the grid connection was removed. Another interesting comparison is between the two different *Full Flex* scenarios, where all flexibility measures were offered, but grid electricity purchasing was the difference. Table 4.3 again indicates that while limited in transmission capacity, the grid access acted as a substitute for the expensive BES, allowing the system to avoid investing in the technology entirely. Additionally, the grid connection also adds the ability to pick and choose from the cheaper electricity source during the hours in which the varying spot price is lower than the constant PPA cost. This effect is seemingly very low, however, most visible in Figure 4.5. This was probably due to limited transmission capacity restricting the quantities that would yield noticeable savings.

The different scenarios were developed to highlight the economic value of incorporating the flexibility measures individually and in unison. Table 4.4 showcases that the flexibility measure with the strongest ability to reduce cost was the H_2 storage. As mentioned above, no optimization selected the smaller hydrogen tanks over the large-scale H_2 LRC, suggesting that the benefit of H_2 storage flexibility (faster charging/discharging) for short-term buffering did not outweigh the cheaper long-duration storage. However, one should point out that it is likely that this dynamic was not captured in the hourly resolution in the model, and that in reality, such tanks would be required to a degree to handle quick and small fluctuations.

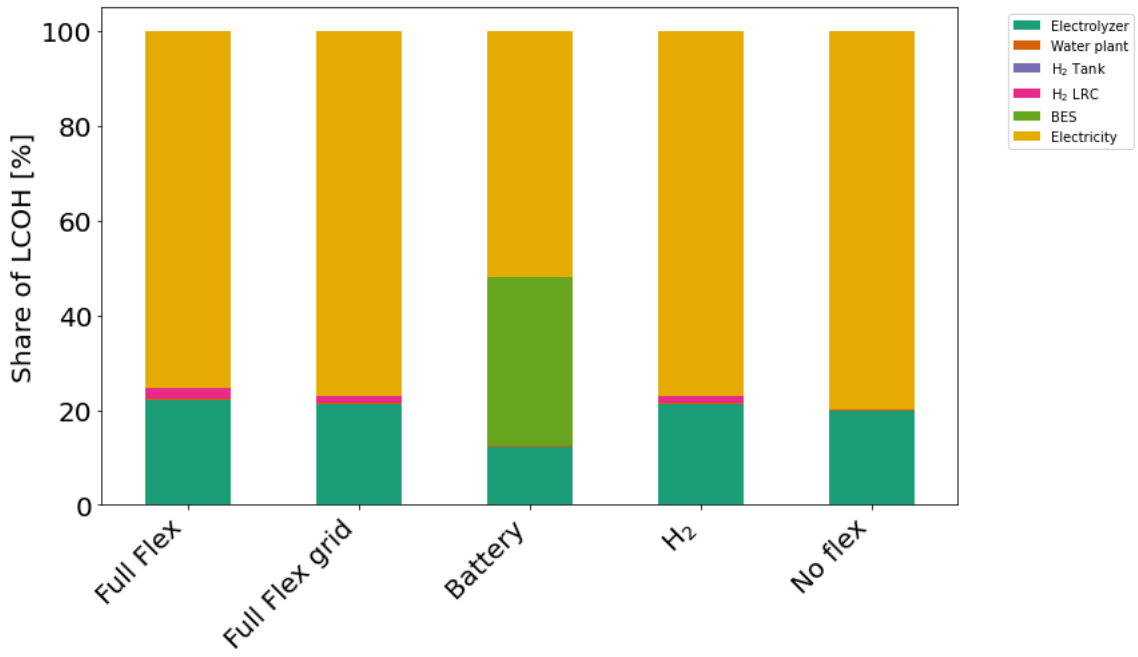

Figure 4.5: Cost distribution of resulting LCOH in each scenario.

However, while purchasing grid electricity offers flexibility and savings, it does come with the downside of slightly reduced RFNBO output, since purchased grid electricity does not count as fully renewable, a dynamic showcased in Table 4.4 along with remaining KPIs. While the RFNBO share does not seem greatly reduced when comparing the scenarios to the *Full Flex* reference case, it does have an impact on the $LCOM_{RFNBO}$ and even more visibly on the produced RFNBO per annum. While the results only capture costs, one should point out that RFNBO is arguably a more highly valuable commodity than the remaining non-certified methanol. So while purchasing from the grid in *Full Flex Grid* reduces the LCOM, this is misleading as in doing so, one reduces the overall profitability and viability of the project due to decreased revenue.

Table 4.4: Resulting KPIs for each scenario

	Full Flex	**Full Flex grid**	**Battery**	$\boldsymbol{H_2}$	**No flex**
Annual cost [M€]	647	642	866	642	639
LCOM [€/ton]	1612	1598	2157	1598	1592
$LCOM_{RFNBO}$ [€/ton]	1612	1642	2252	1642	1730
LCOH [€/kg]	5.76	5.62	8.35	5.62	5.42
RFNBO [kt/a]	402	391	385	391	369
RFNBO share [%]	100	97.3	95.8	97.3	92.0

4.4 Technical Potential to Reduce Costs

In this section, the effects of some key technical parameters will be investigated to assess their impact on the overall system cost and $LCOM_{RFNBO}$. The objective here is to evaluate whether performance improvements could result in significant cost reductions and enhance the economic competitiveness of the product. The analysis will be performed on the *Full Flex* scenario as the reference case.

4.4.1 Electrolyzer Efficiency and CAPEX

With the conclusion that the electrolyzer is the dominating contributor to the system cost, both in terms of investment and electricity consumption, evaluating the effect of capital cost and energy efficiency was deemed interesting. Figure 4.6 showcases the results of the analysis. The expected trends were clear, the LCOM decreases with reduced CAPEX and increased efficiency. Additionally, the economic value of increased efficiency also seems to widen with increasing CAPEX, suggesting that efficiency is more valuable at higher investment levels. Since the hydrogen output is fixed due to fixed carbon feedstock, regardless of efficiency, the main benefit of higher efficiency lies solely in reduced electricity consumption (lower operational costs), and the relative CAPEX benefit diminishes.

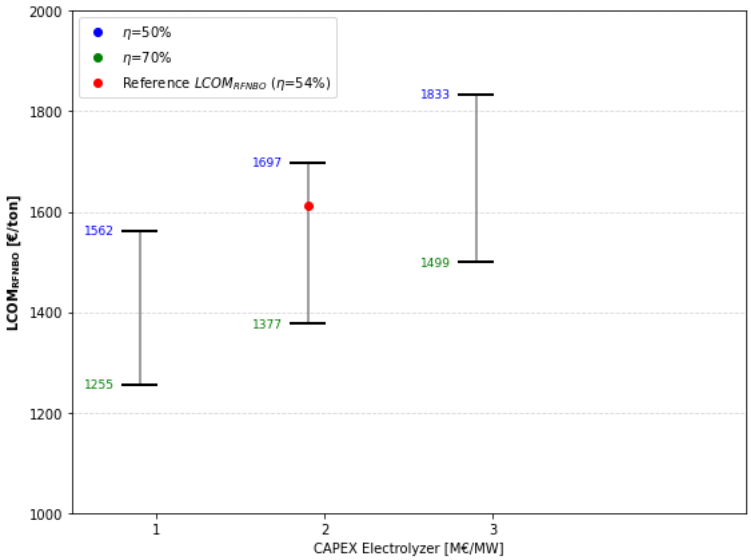

Figure 4.6: Resulting impact on $LCOM_{RFNBO}$ from the varying of PEM efficiency and CAPEX in the *Full Flex* scenario, where the red dot represents the base case.

Clearly, a best-case scenario would equate to a 1255 €/tonne $LCOM_{RFNBO}$, but perhaps more interesting would be to investigate the conditions that would lead to a competitive product. The projected market price could be around 1300 €/tonne for RFNBO in the future [41]. That would suggest that even with the highest of efficiencies, a CAPEX electrolyzer at 3 M€/MW, or a 2 M€/MW at moderate efficiency, would not leave room for net profit at all. However, the data could be useful in the debate of whether technology improvement or technology investment costs

would be the more interesting metric to guide investment decisions. Is it worth waiting for electrolyzer costs to fall, or should one await improved efficiency in PEMs? Figure 4.6 indicates that waiting for the PEM technology to become available at higher efficiency may not be enough for a profitable investment, and additional cost levers are needed for economic viability, either through a great reduction in cost or perhaps technology subsidies.

4.4.2 Alternative Electrolyzer Technologies

Still maintaining that the electrolyzer accounts for the largest impact of any unit, the previous section indicates the viability of the PEM electrolyzer option is constrained by its development. However, as mentioned in 2.5, other electrolyzer options are available. Figure 4.7 shows the results from the model, this time by varying the electrolyzer technology for different CAPEX and efficiencies. The argument here being that AWE, but primarily SOEC, are indicated to have superior efficiencies to the PEM, however, with the downside of being less flexible, either through decreased ramp rates or increased minimum load. Through modeling, one can see how the less flexible technologies fare in an inherently flexible process, and if the consequence of increased need for flexibility measures would offset the economic gain of better performance.

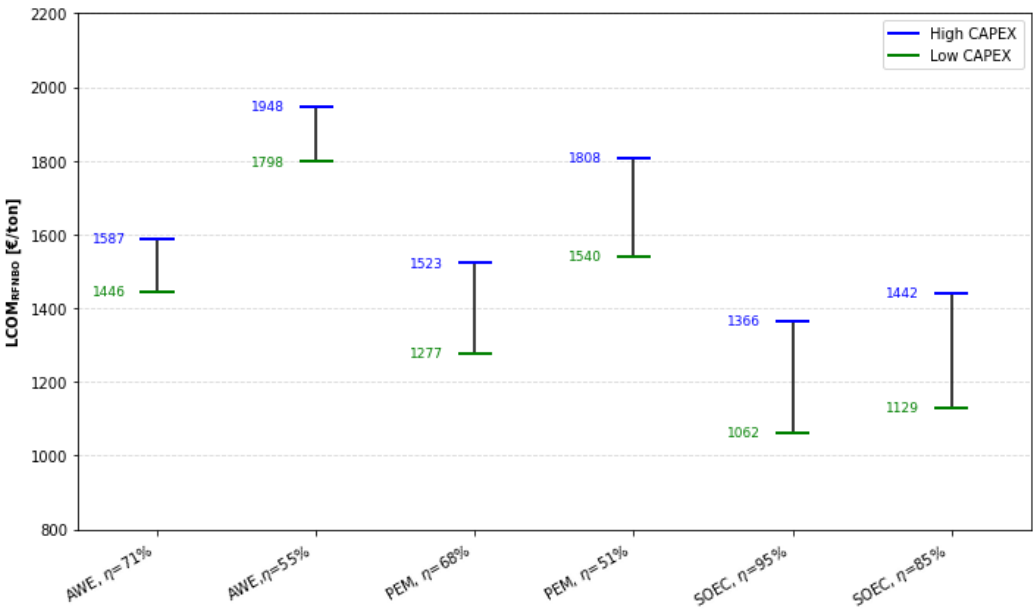

Figure 4.7: Resulting impact on $LCOM_{RFNBO}$ from the varying of electrolyzers types, efficiency and CAPEX in the *Full Flex* scenario.

Given our assumptions for technological data (see Appendix C), the results suggest that the PEM would not be the most cost-beneficial choice of electrolyzer. While there are uncertainties about maturity levels, large-scale applications and system integration, the highly efficient SOEC shows great potential compared to PEM and AWE, even under moderate CAPEX assumptions. On the other hand, comparing AWE to PEM shows the effect of minimum load. The AWE has a higher efficiency

and lower CAPEX, but has a lower ability to operate flexibly, being limited to operating at a minimum load of 20%, negatively impacting the system-wide operation. This consequently requires a substantially larger BES to maintain continuous production, thus increasing the $LCOM_{RFNBO}$. These findings underline the importance of considering both efficiency and integration characteristics when selecting electrolyzer technology.

4.4.3 Methanol Synthesis Flexibility and Conversion Efficiency

The remaining technology worthy of deeper analysis is the methanol synthesis plant, which accounts for around 7 % of the total annual cost. Unlike the PEM, the operational flexibility of the synthesis process is not as well established in literature, and was not determinable through Aspen modeling. As shown in Figure 4.3, the cost contribution from storage flexibility measures was nearly negligible. However, their sizing and operation may be indirectly influenced by the dynamics of the synthesis process. A more flexible plant can reduce the need for oversizing or storage cycling, thus reducing the overall cost. To test this, the system-wide cost impact was investigated by adjusting the minimum load and ramp rates for the synthesis, and showcased in 4.8.

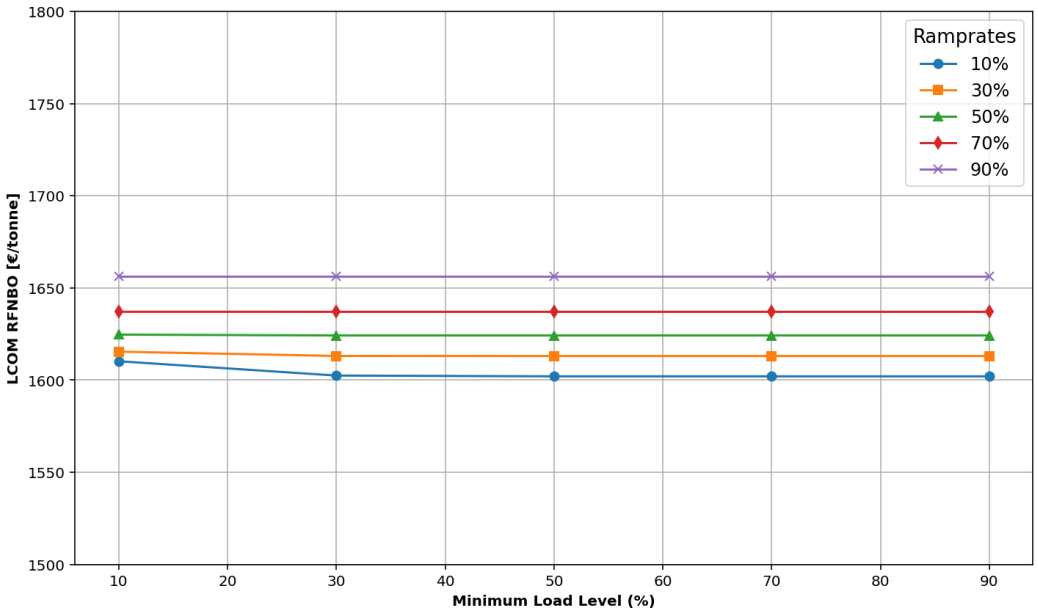

Figure 4.8: Resulting impact on $LCOM_{RFNBO}$ from the varying of ramp rates and minimum load for the methanol synthesis plant in the *Full Flex* scenario.

While one might intuitively expect a more flexible plant to add value to the system, the suspicion was not supported by the data. Interestingly, the sensitivity analysis shows that the flexibility parameters have a near non-existent effect on the result, suggesting that the dynamic capability does not present as a critical parameter or a possible bottleneck in the modeled setup. Worthy of mention is the absence of an economic cost when the technical parameters were adjusted in the model. The

simplification does not capture the fact that in a real-world design, a more flexible and sophisticated technology would come at a higher investment and operational cost. The result is valuable through a system design perspective, implying that investing in a highly flexible methanol synthesis plant may not be cost-effective, and that additional capital may be better allocated to other parts of the supply chain.

Another aspect of the synthesis worth investigating is the conversion efficiency, in this case modeled as the share of the input successfully converted into product contra turning into emissions. While not explored thoroughly through detailed modeling in this work, the implications are relatively straightforward. An increase in conversion does not reduce the overall need for hydrogen, carbon or electricity input in any unit, nor does it affect capacities or operation of units prior in the supply chain. Instead it only leads to a higher product yield per input. The effect on $LCOM_{RFNBO}$ can be more easily understood through the calculation in Equation 3.40, where an increase in conversion would primarily increase the denominator by amplifying product output, and simultaneously decreasing the nominator through reduced emission costs.

The gains in levelized cost scale linearly, as no changes in system behavior occurs. As such, while the increased conversion is desirable in practice, it does not present any complex tradeoffs or nonlinear dynamics that would justify detailed analysis. One could imagine that a more sophisticated technology would come at an increased expenditure. For example, increasing the conversion from 92% to 94% is usually far more technically challenging and capital intensive than improving from 52% to 54%. However, considering that the synthesis is such a small fraction of the capital costs, and operational expenditures of electricity being minimal compared to the electrolyzer, it stands to reason that any improvements would be desirable and economically justifiable.

4.5 Sensitivity to Intermittency and Electricity Costs

Previous sections confirm that the production cost of RFNBO is highly correlated to electricity, yet while clearly important, the impact on the overall system cost may not solely be dependent on the electricity price, but also the degree of intermittency of wind power in the modeled year. To investigate this effect, one can vary the PPA cost for different years with higher and lower wind availabilities. Figure 4.9 illustrates the results of how they impacted the $LCOM_{RFNBO}$. To capture the broadest effects, the best (2015, CF = 65.2%) and worst (1980, CF = 50.5%) wind years were selected for each PPA cost.

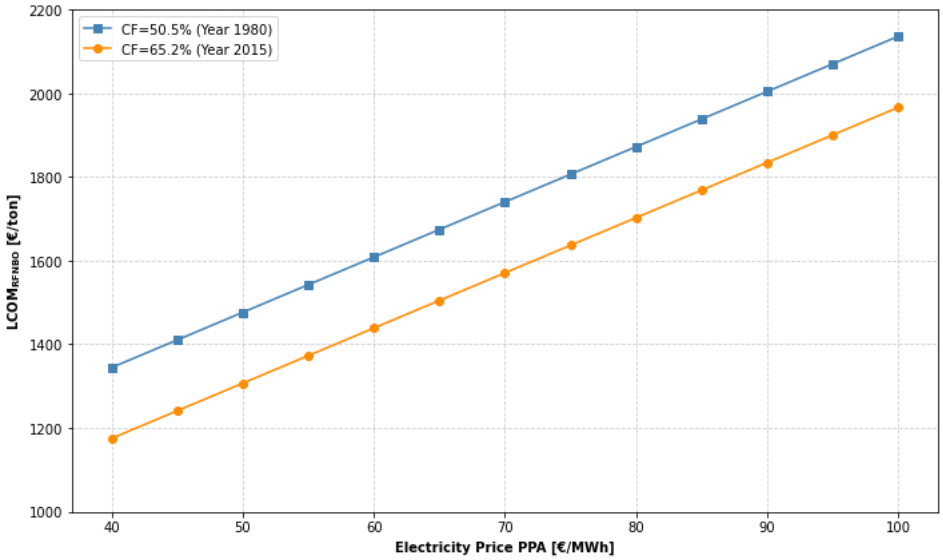

Figure 4.9: Resulting impact on $LCOM_{RFNBO}$ from varying electricity price and wind capacity factors (CFs) in the *Full Flex* scenario.

The result indicates a consistent linear impact between the electricity procurement cost and the resulting levelized cost. Furthermore, the influence of wind availability is seemingly steady within the investigated interval. While the effects of electricity price are straightforward, the cost reduction followed by higher wind capacity factor is primarily driven by reduced system intermittency and therefore reduced need for surrounding flexibility measures. In better wind years, the degree of low wind events lessens, leading to the model concluding that there is less of a need to store energy or overproduce and store hydrogen. The result being a gradually more uniform production throughout the year, allowing for cost reductions through smaller storages and less oversizing of key technologies, as the peaking events are reduced in amplitude. In contrast, the worst wind years require increased buffer capacity for longer periods of low wind power production, driving up capital expenditures. As such, one can conclude that while the PPA price is a primary cost driver, the effect of intermittency unveils additional system-wide costs, not captured by the PPA.

This raises an important aspect of system design for projects with an intermittent nature that need to last for years or decades. The model only considers the data with which it is fed, in this case, over a single year. But if the system is supposed to remain operationally sufficient across all of the years of its technical lifetime, it should be dimensioned for the worst-case weather conditions. Yet in doing so, one has then overinvested in capacity for the average years, and is underutilizing the investments during favorable periods. But by instead modeling for average conditions, one opens up to the risk of production shortfalls during the inevitable poor wind year.

4.6 Import in the Supply Chain

Section 4.5 implies that wind conditions have a considerable effect on both the PPA price and system-wide investments. While one could investigate adding or changing to other renewable energy sources in the system, another mitigation strategy could be geographic diversification. By relocating the system to regions with better and more stable wind profiles (or abundant access to solar power), one can lessen the cost burden along the arguments previously covered. However, even if we disregard all regulatory and administrative barriers that undoubtedly come with foreign production, new trade-offs would be introduced.

While a certain region could highly improve on the current electricity procurement, one challenge with relocating the entire supply chain would be finding an equally sizable quantity and concentrated source of biogenic CO_2 (or DAC facility) that complies with the regulatory criteria for RFNBO classification. Otherwise, moving the entire supply chain could theoretically include the long-distance transportation from captured carbon at Lysekil, but this would be highly costly and logistically complex, and as such, excluded as an option. Instead, this report will only consider importing a part of the supply chain, hydrogen, removing the need for electrolysis while still keeping the methanol synthesis on the west coast of Sweden.

As concluded in Figure 4.5, all scenarios indicate that the LCOH is predominantly affected by electricity prices, which are linked to the LCOE that vary geographically between generation technologies and regional conditions. An example being offshore wind, where the weighted average for LCOE in China was 25 % lower compared to Europe as a whole [94]. For example, the cost of producing H_2 in Germany and Norway, where the power was supplied from the electricity grid, resulted in an LCOH of 12.51 and 9.70 €/kg, respectively [95]. A notable downside is that, even if the grid meets the RFNBO criteria, grid fees and energy taxes are added to the cost. In Spain, an even lower LCOH can be achieved by supplying energy from solar PVs, decreasing to 6.19 € per kg H_2 in such a setup [95]. For reference, the levelized cost for blue H_2 (produced from SMR) in Europe is on average 4.41 and 3.76 € per kg H_2 for with and without a carbon capturing unit, respectively [96]. But these values only showcase the current landscape. According to the International Energy Agency, the LCOH by 2030 can be as low as 1.8 to 2 €/kg in regions such as Australia, India, and Morocco [97]. In areas such as Argentina and Chile, they can be even lower, reaching values down to 1.5 €/kg H_2 compared to Sweden, where the LCOH is forecasted to be more than twice as high.

So, to evaluate the impact of importing hydrogen to a potential Lysekil site, Australia, Morocco and Chile were selected as interesting regions to investigate, with LCOH values as discussed above. However, one should also add on top the estimated cost of transporting liquefied hydrogen to Northern Europe, which are estimated to be 1.5, 2.6, and 3.7 €/kg H_2 for North Africa, Chile, and Australia, respectively. These added costs includes all segments that come along with import, including liquefaction, transport, and distribution cost [91]. These were incorporated in Figure

4.10, which showcases what LCOH is achievable in local production when varying through a series of PPA cost scenarios, with the color bar indicating what the resulting $LCOM_{RFNBO}$ would be. However, the plot also includes the cost at which liquid hydrogen could be imported from the H_2 import regions.

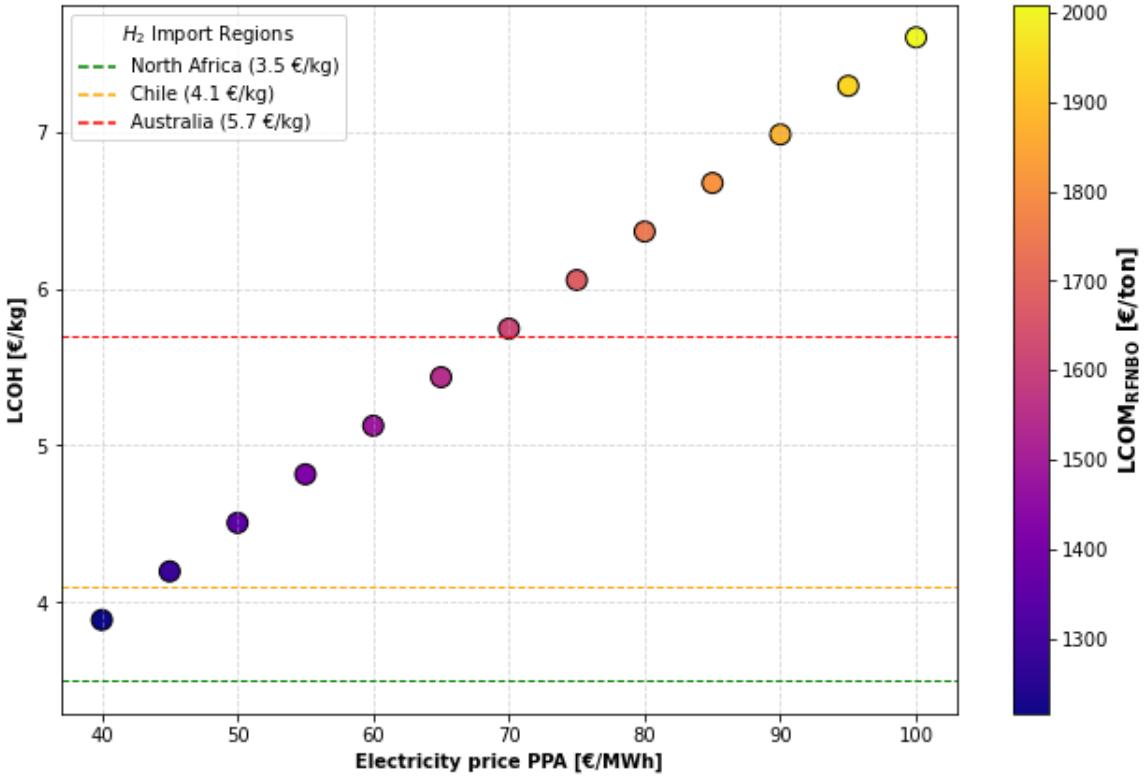

Figure 4.10: Cost comparison between importing hydrogen or local production through varying PPA price, along with the effect on $LCOM_{RFNBO}$.

The results show that imports from Australia are equivalent to domestic production at an electricity price of 70 €/MWh, Chile at roughly 43 €/MWh, and the cheapest option is North Africa in the lower 30s. These intersecting points should be interpreted as up until what PPA price domestic production is preferable, and beyond that point, imports become more favorable.

However, one should also point out the uncertainties. First of all, the volumes of hydrogen required are so massive (+100 kt/a) that they could exceed the available supply or cause supply chain issues, increasing the price from what is displayed. There is also the aspect of transportation. The costs in the figure include the liquefaction and transportation of hydrogen in specialized freight ships. But these ships are not abundant, and not easily obtained or rented. This may prove such large-scale transportation infeasible. Other transportation methods through hydrogen carriers could show more promise. For example, Ammonia (NH_3) is liquid at ambient temperatures and as such does not require the added complexity in freight transport. However, ammonia is not yet used at scale as a H_2 carrier, mainly due to energy losses in the intensive conversion and the reconversion process of H_2 to NH_3. Addi-

tionally, there are difficulties during storage and transport, as the compound is toxic and corrosive, which cause safety challenges[98]. Another option would be through so-called *Liquid Organic Hydrogen Carriers* (LOHCs), binding hydrogen chemically to carbon (or carbon and oxygen) to create liquids at ambient temperatures. This could, for instance, be methanol or other alcohols, which have the upside of easier handling and more established transportation methods, but would require a source of biogenic carbon in the importing region at an added cost, with arguments laid out against earlier.

Beyond the techno-economic aspects, one should also consider the strategic and compliance concerns. A core part of the ReFuelEU regulation is the close monitoring and strict traceability of electricity on an hourly basis to guarantee the RFNBO certification. The criteria might be tougher to ensure for imported hydrogen, especially if the prior parts of the supply chain (e.g the renewability of electricity or electrolyzer certification) can not be verified under EU standards. Additionally, having to rely on imports for a fundamental component of one's production from international regions introduces energy security risks and vulnerabilities. To reduce risks, an import strategy should be carefully structured to include diversification, rather than relying solely on imports from the cheapest region. By spreading imports across multiple regions, one can mitigate supply chain disruptions beyond direct control and reduce the vulnerability associated with geopolitical risks, market volatility, and competing tariffs. To conclude, while importing hydrogen may present cost advantages under viable pathways with favorable conditions, it introduces significant trade-offs related to regulatory compliance, operational control, and long-term system stability.

4.7 Economic Feasibility and Competitiveness

With all results presented, this final section can analyze the systemic economic factors that affect the financial viability of e-methanol production, under the conditions modeled in the *Full Flex* scenario.

As mentioned previously, the cost for conventional methanol varies between 370 to 700 € per ton of methanol. That methanol is mainly produced using natural gas through steam methane reforming, which results in a production cost of roughly 150 € per ton of methanol [99]. However, the production cost of e-methanol is estimated to be approximately 1000 € per tonne, but is highly dependent on the LCOH, or in other words, dependent on where it is produced [99]. Furthermore, the International Renewable Energy Agency has estimated that when when biogenic CO_2 is utilized, the production cost falls in the range of 800–1600 €/tonne, with the expectation that this cost could decrease to 630 €/tonne as the technology matures [31].

In the base case scenario, using the parameter value presented in the various tables in section 3.3, the resulting $LCOM_{RFNBO}$ amounted to 1612 €/tonne, with the RFNBO-compliant share accounting for the totality of the produced product. Before considering any cost-reducing measures, one can recognize that production at Lysekil will be outside the upper end of the estimated interval for northern Euro-

pean production, a not-so-promising sign for economic viability. In northern Europe, Concawe calculated the cost of e-methanol (2020 levels) to be 1931 €/tonne, but decreasing to 1303 €/tonne in 2030 and remaining at that production cost level even in the year 2050 [91]. However, according to S&P Global, the market price for e-methanol is expected to be 2238 €/tonne between 2025 and 2033, but a projected decrease to 1325 €/tonne between 2034 and 2050, signaling that the gradual increase in demand through the ReFuelEU regulation will be outweighed by an abundance in increasing supply [41].

While these static comparisons provide a telling glimpse, a more comprehensive assessment of economic viability requires considering how profitability alters or evolves over time. To evaluate this, the NPV metric is used, capturing both the timely value of money and total revenue of the project over its lifetime.Figure 4.11 illustrates how the project's NPV would evolve over its technical lifetime for varying constant market prices for e-methanol, under the common assumptions of a three-year assumption for construction, a 10% discount rate, and a 25-year operational lifetime.

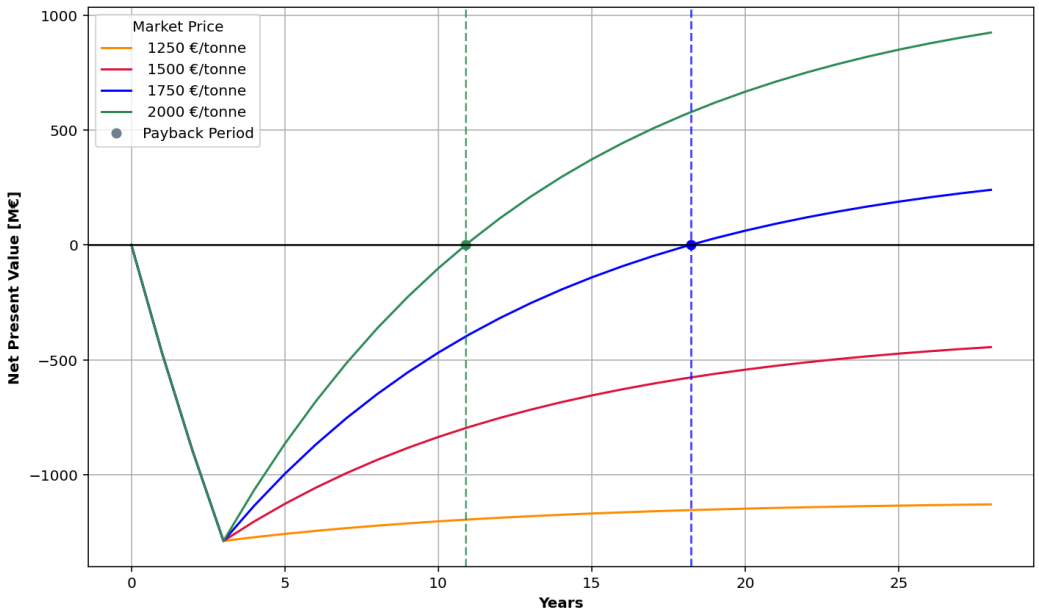

Figure 4.11: NPV curve of the project in the *Full Flex* scenario, based on different e-methanol prices.

The results indicate that if the market price would remain around 2000 €/tonne, an optimistic assumption, the project would quickly reach payback in around eight years of operation, leading to a highly positive NPV after 25 years. A more probable scenarios is around the ranges of 1750 €/tonne. In the latter, the payback period is delayed to around 15 years, and notably reducing the NPV after operational lifetime. So while still profitable, the limited upside may dissuade investors. In the two lowest priced scenarios, the breakeven point is never reached within the projects technical lifetime, indicating that these price levels would not make the investment financially viable under the assumed conditions. This highlights that the market price must consistently stay above €1750/tonne for the investment to be considered, and to

ensure that profitability is not fragile.

Besides the influence of the products market price, a second driver of a project's NPV is the discount rate. In simplified terms, the parameter reflects the minimum return that an investor or project developer would need to justify committing capital to a specific investment, in contrast to investing in a safer asset. But embedded in that rate is also so-called a risk premium, an increased rate reflecting an expected greater return as compensation for taking on greater uncertainty [100]. One must recognize that regionally, near the first of its kind, offshore wind-powered e-methanol production, is a risky venture. This aspect is especially relevant when considering the regulatory uncertainty around RFNBO, the supply chain requiring underlying technologies that are still maturing, and the absence of long-term offtake agreements. However, it is determined, riskier ventures must offer higher potential returns, and economic feasibility must be considered with an appropriately high discount rate acting as a benchmark against project and systemic risks.

Figure 4.12 shows the sensitivity of NPV to different discount rates, assuming a fixed market price of 1750 €/tonne under the *Full Flex* scenario, and uses the same cost structure of three year investment period followed by 25 years of operation.

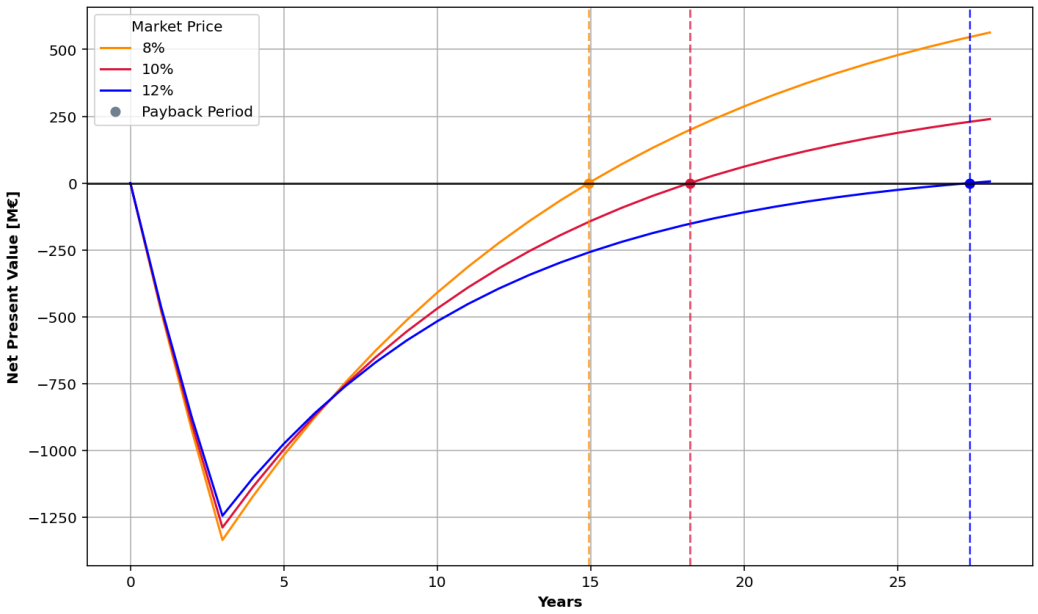

Figure 4.12: NPV curve of the project in the *Full Flex* scenario, based on different discount rates. Market price set to 1750 €/t

As shown in the figure, even single percentage changes have major impacts on the long-term profitability. At an optimistic discount rate of 8%, the payback period is reached around year 12 of operation, with a moderately high total NPV. However, since the investment costs is assumed to be loaded upfront during the construction years with the returns spread over a 25-year period, the discount rate has a significant impact on economic feasibility, with a higher rate penalizing future cash flows [101]. This concept can be seen in the 12% curve, where the project's final NPV

is close to zero and just barely reaching the break-even point, with the flattened curve being a great presentation on how higher discounting rates sharply reduce the present value of distant future cash flows.

The result highlights a fundamental challenge. Due to RFNBO fuels not having reached commercial maturity and the policies in question lacking clarity, one can confidently state that there will be uncertainty in the RFNBO market environment. As such, the discount rate for these types of projects is likely to be elevated, hurting economic viability. Consequently, any real investment decisions will require some mechanisms that will reduce the overall perceived risk of the venture, and in turn, the applied discount rate. This could be instruments such as long-term offtake agreements that guarantee long-term cash flow or subsidies of some kind that would lessen the economic burden will be essential to making the commitment attractive to the decision makers.

5
Discussion

There are several uncertainties that influences the implementation of local large-scale e-methanol production. These involves the market, energy security aspects as well as policy and international trade.

5.1 Market Uncertainties

As concluded, large-scale e-methanol production is a very capital-intensive investment, especially for Preem's ambitions, as their production goal would be sufficient to supply half the domestic flight demand in Sweden in 2023, and then some. These kinds of projects require a certainty in future revenues to be financially justifiable. As mentioned in the introduction, in this context, that would imply that offtake agreements are essential to reduce risk. However, aligning production deployment with the gradually evolving mandates from ReFuelEU that initiate the demand to match the supply, is a complex task. The case of Preem Lysekil depicts this challenge. Yes, the production volumes are sufficient to meet half the Swedish aviation sector's e-SAF demand, but the demand is not there in operational year one. This creates a temporal mismatch between supply capacity and the regulatory-influenced demand. That means that for Preem to be profitable, they either need to time the market, or establish several offtake agreements, which adds further complexity and risk.

Another factor that adds complicates timing the market, is the uncertainty and evolving maturity of and between technologies. The electrolyzer, a primary cost driver, is in an ongoing transition. While the results showed that even with a lower investment cost and increased η for the PEM help lower cost, they would still not make local e-methanol production cost-competitive (see Figure 4.6).

However, the biggest potential seems to appear when investigating other technologies, most notably the less mature SOEC, which offer significantly higher efficiencies. It is worth noting that because of its lower TRL, it is probably not commercially available as a large-scale application for Preem to become early actors on the market, but one could imagine a scenario where Preem could enter the market later when the SOEC matures, and have an advantage in production cost against older producers on the market. The same argument could be made for some of the other units, including but not limited to the carbon capture unit, which accounts for a notable share of the $LCOM_{RFNBO}$.

Another layer of uncertainty lies in electricity procurement. The study assumed a PPA cost of 70€/MWh, roughly reflecting the LCOE of offshore wind, but could end up being higher in reality since additional cost would be required to account for surrounding expenditures, like the direct transmission line, energy tax, and practicalities. Furthermore, just as Preem faces risks, the wind farm owner must ensure their own profitability, which could potentially require a higher PPA, significantly affecting the studied system configurations cost-competitiveness.

Lastly, the unpredictability in market price dynamics adds further volatility. Previous sections discuss that current projections suggest that the market price could be upwards to 2000 €/tonne through the early 2030s, but leaving little room for profit when sharply reducing to roughly 1300 €/tonne thereafter, once supply scales up. On the other hand, projects are being postponed or canceled, suggesting that scale up may be delayed, which could leave Preem as one of few actors on the unsaturated market, resulting in promising profitability conditions.

Viewing these aspects collectively, the uncertainties around timing suggest that delaying investment in the range of several billion euros and not make any hasty decisions, could potentially favor Preem. But while entering under clearer market conditions, a stronger policy environment and more affordable technologies might seem lucrative, it is often the early movers, willing to accept greater uncertainty, that can capture the most value before the market saturates and margins tighten.

5.2 Energy Security

Energy security is a crucial aspect and cannot be understated, especially if looking at the past couple of years (2020-2024) in Europe. It is crucial to have reliable and access to affordable energy, but in the same time not risk the supply chain disruption and the following vulnerability that comes with that. There are several advantages to importing part of the supply chain, apart from reducing cost. For example, less complexity and unit capacities need to be put in place at the refinery, which could be restricted to space as well as environmental permissions. It could be shown in Figure 4.10 that importing H_2 would be an interesting pathway to investigate further, since the largest cost share of $LCOM_{RFNBO}$ would have been outsourced. Since there are such large volumes of H_2 that would need to be imported, most likely several regions would be involved. This can decrease the risk, since you are less dependent on one specific import region, but it also adds risk because of the added complexity. Transporting H_2 is not a developed market yet, which also adds uncertainty and risks. Regarding energy security, further work is needed to first of all see which regions would be interested and how potentially such a setup would look like, since there could be challenges with the import, either related to the transport or the international production. timing, risk etc.

5.3 Policy Barriers and Opportunities

The cheapest scenario in order to produce the most RFNBO is the *Full flex* scenario, but since the other scenarios were not far off, there are potentially improvements related to the utilization of the grid that can be made. As of today, the implementation and operation to fulfill the REfuelEU Aviation policy does not come easily. Even if this project did not dive into different ways of utilizing the grid, the regulation does not promote the expansion of electrofuels. This is mainly because of the requirements of a new renewable plant that needs to be in place within a certain time frame for the fuel production plant. Often projects get delayed and to have a requirement such as the installation generating renewable electricity that needs to be in operation not earlier than 36 months before the fuel production might make things more complicated than necessary. Also, the extensive requirements to be able to consume electricity from the grid. More specifically, the measurement of the GHG emissions two years prior to the current year, where new installations of renewable energy can take place at a much faster pace, leading to an outdated measurement.

One thing that is specific for Sweden is the negative electricity prices, which accounted for almost 10 % of the hours in 2024 in SE3. This is a great opportunity to act like an energy sponge and absorb excess electricity (by increasing production) instead of curtailment or utilization of other demand-side management strategies. In such a situation, the policy promotes this kind of action if it can be shown that it solves the experienced imbalance from the Swedish transmission system operator (Svenska Kraftnät). This would potentially encourage more renewable energy installations in the energy system, since excess renewable energy production can be used to produce e-fuels.

5.4 Import and International Production

If the conclusion above stands, producers should investigate the possibility of moving parts of the production to these regions with cheaper renewable electricity, to stand on the same footing as competitors. The results analyze some options for the import of H_2. Given our assumptions about transportation costs, cost-effective solutions are available. Out of the three options, Australia was deemed equatable to local production at 70€/MWh, but both Chile and North Africa suggested fascinating opportunities, and it stands that even more regions could be feasible.

While section 4.6 investigates the import of hydrogen, section 3.5 explains that a large share of the LCOH is due to the expensive liquefied H_2 transportation cost (roughly 43, 63 and 65% for North Africa, Chile, and Australia respectively). An alternative approach could be to produce the e-methanol abroad directly alongside the hydrogen. Assuming the MtJ process is still kept in Sweden, importing of e-methanol could be cheaper than producing it on-site. The argument here is that methanol as a compound is easier to transport, due to it being liquid in ambient temperatures, and having energy losses as liquefaction of hydrogen would.

However, this would complicate the supply chain as it is necessary to have captured CO_2 near the fuel production facility (either through DAC or biogenic carbon through industrial processes), to avoid the costly capture and transportation from the Lysekil refinery. This adds another level of complexity, as a region with cheaper electricity might not be the cheapest production site, as it may have a more costly or even more limited carbon source. This would merit further study, but the literature work did not find any accurate data for e-methanol production cost in these regions, and there could be uncertainties if they would comply with the non-biological origin of CO_2, which after 2040 needs to be biogenic or from DAC. Worth noting is that due to the potential of producing H_2 at a low cost, it is likely that the e-methanol will be substantially lower, since the LCOH accounts for more than 70 % of the cost.

5.5 Further Work Suggestions

During the study, several areas were excluded, but further investigation could provide valuable insights that would strengthen the conclusions of the study.

One such aspect was system scalability. Approximately 83% of Marelds available wind power is utilized in the *Full Flex* scenario, but one could imagine a scenario where a favorable market environment would tempt the decision makers to increase production. An increase in carbon feedstock, could easily push the utilization to 100%, capping their ambitions. However, even modest upscaling ambitions could lead to disproportionately increased investments in battery or electrolyzer technologies to efficiently allocate the limited energy. On the other hand, investigating whether an increase in allocated wind farm capacity from the Mareld site could reduce the need for flexibility, and in turn reduce the levelized cost, would also be interesting.

Secondly, since the report concluded that electrolyzer technology, efficiency and CAPEX played an immense role in the economic viability, future work should investigate the economic impact and regulatory limits of sourcing electrolyzers from non-EU markets. This would be particularly interesting for China, where capital costs are reportedly significantly lower, but could be hindered by EU restrictions.

Finally, the analysis could stand to benefit from a full life cycle assessment. Making sure that the total emissions, including upstream emissions and the environmental impacts of the product, do not exceed the set threshold of 28 gCO2eq/MJ, since this study only looked at emissions from the production system. This could also be important in determining the viability of grid power, since the share of renewables is directly correlated, and in turn would inform whether there is a need for incorporating guarantees of origin for the grid power.

6
Conclusion

The objective of this thesis was to investigate the technical and economic feasibility of local e-methanol production, located on the west coast of Sweden, as part of a supply chain for a specific sustainable aviation fuel that complies with the recently implemented initiative called ReFuelEU Aviation, which outlines a gradual increase in these aviation fuels to reduce emissions within the aviation sector.

The production of local e-methanol does not clearly indicate that the studied system would be cost-effective compared to future estimated market prices. While certain conditions could make it viable, other options should be considered. This study highlighted the importance of having large-scale H_2 storage for economic feasibility, and the estimated size would also be technically possible, but further investigations related to geological limitations need to be performed. There are also uncertainties regarding the interpretation of the policy, such as the use of the grid and the requirement that new renewable power installations must be commissioned no earlier than 36 months before fuel production, which could affect the development of e-methanol.

The cost of producing e-methanol in the base case was 1394 €/t, with a corresponding hydrogen production cost of 5.72 €/kg, compared to blue hydrogen in Europe, which averages 3.76 €/kg. Hydrogen contributed 60% of the e-methanol production cost, making it a key cost driver. Since hydrogen production is directly correlated with electricity prices, the most important factor influencing the cost of e-methanol is the electricity price itself. This makes electricity a decisive factor in determining whether local fuel production can be cost-competitive. Importing hydrogen from regions with lower electricity costs showed potential to substantially reduce methanol production costs. However, to consider this a viable option, further investigation is needed to minimize potential energy security risks.

There are also several uncertainties beyond those mentioned above. The results showed that other electrolyzer technologies could make local e-methanol more cost-competitive, but technological readiness and market development remain uncertain. The future market price of methanol has been estimated, but it could change significantly in the coming years, depending on how the planned projects evolve. Since these types of investments involve billions of euros, the results are not convincing enough to recommend local methanol production as a cost-effective investment on the west coast of Sweden.

Bibliography

[1] European Commission, "2050 long-term strategy," 2023. Accessed: 2025-05-13.

[2] European Energy, "E-methanol: A game changer for decarbonising heavy transport and industry," January,2025. Accessed: 2025-03-10.

[3] International Energy Agency, "The role of e-fuels in decarbonising transport," 2023. Accessed: 2025-04-01.

[4] European Commission, "ReFuelEU Aviation," 2025. Accessed: 2025-03-10.

[5] European Union Aviation Safety Agency, "Fit for 55 and refueleu aviation," n.d. Accessed: 2025-01-23.

[6] U.S Department Of Energy, "Sustainable aviation fuel," December 20, 2023. Accessed: 2025-01-28.

[7] M. Prussi, U. Lee, M. Wang, R. Malina, H. Valin, F. Taheripour, C. Velarde, M. D. Staples, L. Lonza, and J. I. Hileman, "Corsia: The first internationally adopted approach to calculate life-cycle ghg emissions for aviation fuels," *Renewable and Sustainable Energy Reviews*, vol. 150, p. 111398, 2021.

[8] European Commission, "ReFuelEU Aviation," n.d. Accessed: 2025-02-03.

[9] European Union, EUR-Lex, "Regulation (EU) 2023/2405 of the European Parliament and of the Council of 18 October 2023 on ensuring a level playing field for sustainable air transport (ReFuelEU Aviation)," October 21, 2023. Accessed: 2025-02-03.

[10] European Commission, "Directive (EU) 2018/2001 of the European Parliament and of the Council of 11 December 2018 on the promotion of the use of energy from renewable sources," 21-12-2018. Accessed: 2025-02-03.

[11] Liquid Wind, "eMethanol," n.d. Accessed: 2025-04-01.

[12] Methanol Institute, "Carbon Footprint of Methanol," 2022. Accessed: 2025-04-01.

[13] F. V. Vazquez and D.-A. Strittmatter, "Why e-methanol is a game changer for decarbonizing shipping and industry," 2025. Accessed: 2025-03-31.

[14] FuelCellsWorks, "E-Methanol from Kassø Gets First-Ever EU Certification on Green Fuels," 2025. Accessed: 2025-05-08.

[15] Hydrogen Europe, "Kassø power-to-x achieves milestone with first production of green hydrogen," 2025. Accessed: 2025-04-01.

[16] Tidningen Energi, "Ørsted lägger ned satsningen på e-metanol i Örnsköldsvik," 15-08-2024. Accessed: 2025-02-03.

[17] Hydrogeninsight, "Government-backed green hydrogen-to-methanol pilot in belgium scrapped due to 'escalating costs'," 02-02-2024. Accessed: 2025-02-03.

[18] Preem, "Ny historisk affär för Preem: Säljer egentillverkad HVO100 till Nederländerna," December 20, 2023. Accessed: 2025-01-23.
[19] Preem, "A climate-neutral value chain by 2035-with the climate target in mind, we are fundamentally changing our business.," n.d. Accessed: 2025-01-23.
[20] Preem, "Vi utvecklar, producerar och säljer biodrivmedel till den svenska marknaden och utomlands," n.d. Accessed: 2025-01-28.
[21] Preem, "Två av Europas modernaste raffinaderier ligger i Göteborg och Lysekil," n.d. Accessed: 2025-01-23.
[22] Preem AB, "Investing in renewable aviation fuel and renewable diesel," 2025. Accessed: 2025-05-14.
[23] Preem, "I år fördubblar vi produktionen av förnybara drivmedel," n.d. Accessed: 2025-01-21.
[24] Cision News, "Vattenfall och Preem ska undersöka storskalig utfasning av fossila bränslen med hjälp av havsbaserad vindkraft och vätgas," June 27, 2022. Accessed: 2025-01-28.
[25] Elevate Aviation Group, "Promise and Shortcomings of Sustainable Aviation Fuel (SAF)," n.d. Accessed: 2025-01-23.
[26] SP Global, "SAF production to triple to 1.5 mil mt in 2024 but progress slow: IATA ," December 6, 2023. Accessed: 2025-01-22.
[27] World Economic Forum, "Sustainable aviation fuels: Offtake manual," 2023. Accessed: 2025-01-23.
[28] M. S. Taslimi, A. Khosravi, Y. K. Nugroho, and N. G. M. Rytter, "Optimization and analysis of methanol production from co2 and solar-driven hydrogen production: A danish case study," *International Journal of Hydrogen Energy*, vol. 69, pp. 466–476, 2024.
[29] S. Pratschner, F. Radosits, A. Ajanovic, and F. Winter, "Techno-economic assessment of a power-to-green methanol plant," *Journal of CO2 Utilization*, vol. 75, p. 102563, 2023.
[30] Methanol Institute, "About methanol." Accessed: 2025-03-05.
[31] International Renewable Energy Agency (IRENA), "Innovation outlook renewable methanol," 2021. Accessed: 2025-03-05.
[32] L. Lv, L. Zhu, H. Li, and B. Li, "Methanol-power production using coal and methane as materials integrated with a two-level adjustment system," *Journal of the Taiwan Institute of Chemical Engineers*, vol. 97, pp. 346–355, 2019.
[33] N. J. Azhari, D. Erika, S. Mardiana, T. Ilmi, M. L. Gunawan, I. Makertihartha, and G. T. Kadja, "Methanol synthesis from CO2: A mechanistic overview," *Results in Engineering*, vol. 16, p. 100711, 2022.
[34] K. Stangeland, H. Li, and Z. Yu, "Thermodynamic Analysis of Chemical and Phase Equilibria in CO2 Hydrogenation to Methanol, Dimethyl Ether, and Higher Alcohols," *Industrial & Engineering Chemistry Research*, vol. 57, no. 11, pp. 4081–4094, 2018.
[35] M. Bowker, "Methanol Synthesis from CO2 Hydrogenation," *ChemCatChem*, vol. 11, no. 17, pp. 4238–4246, 2019.
[36] S. Ghosh, L. Olsson, and D. Creaser, "Methanol mediated direct CO2 hydrogenation to hydrocarbons: Experimental and kinetic modeling study," *Chemical Engineering Journal*, vol. 435, p. 135090, 2022.

[37] M. K. Koh, Y. J. Wong, and A. R. Mohamed, "The effect of process parameters on catalytic direct CO2 hydrogenation to methanol," *IOP Conference Series: Materials Science and Engineering*, vol. 1195, p. 012034, oct 2021.

[38] F. Pontzen, W. Liebner, V. Gronemann, M. Rothaemel, and B. Ahlers, "Co2-based methanol and dme – efficient technologies for industrial scale production," *Catalysis Today*, vol. 171, no. 1, pp. 242–250, 2011.

[39] V. Ballal, O. Cavalett, F. Cherubini, and M. D. B. Watanabe, "Climate change impacts of e-fuels for aviation in Europe under present-day conditions and future policy scenarios," *Fuel*, vol. 338, p. 127316, 2023.

[40] H. Ababneh and B. Hameed, "Electrofuels as emerging new green alternative fuel: A review of recent literature," *Energy Conversion and Management*, vol. 254, p. 115213, 2022.

[41] S&P Global Commodity Insights, "EU regulations to close price gap between sustainable, fossil methanol," 2024. Accessed: 2025-03-10.

[42] Methanex Corporation, "Methanol pricing," 2025. Accessed: 2025-03-10.

[43] M. Fasihi and C. Breyer, "Global production potential of green methanol based on variable renewable electricity," *Energy & Environmental Science*, 2024. Received 4th September 2023, Accepted 4th April 2024, First published on 29th April 2024, © The Royal Society of Chemistry 2024.

[44] The European Parliament, "Directive (eu) 2023/2413 of the european parliament and of the council of 18 october 2023 amending directive (eu) 2018/2001, regulation (eu) 2018/1999 and directive 98/70/ec as regards the promotion of energy from renewable sources, and repealing council directive (eu) 2015/652," 2023. Officiell journal L, 31.10.2023 EN.

[45] European Commission, "Commission Delegated Regulation (EU) 2023/1185 of 10 February 2023 supplementing Directive (EU) 2018/2001 of the European Parliament and of the Council by establishing a minimum threshold for greenhouse gas emissions savings of recycled carbon fuels and by specifying a methodology for assessing greenhouse gas emissions savings from renewable liquid and gaseous transport fuels of non-biological origin and from recycled carbon fuels." Official Journal of the European Union, 2023. Accessed: 2025-03-24.

[46] Fortum Adp, "PPA: stability and carbon-free electricity through long-term power purchase agreements," n.d. Accessed: 2025-03-04.

[47] Svensk Vindenergi, "PPA – ett långsiktigt avtal om inköp av el," n.d. Accessed: 2025-03-04.

[48] Enel X, "PPAs: delivering sustainable energy for every enterprise," n.d. Accessed: 2025-03-04.

[49] Renewables Valuation Institute, "Pay-as-produced PPA vs. Baseload PPA," 4 November, 2023. Accessed: 2025-03-04.

[50] National Renewable Energy Laboratory, "The role of energy storage in decarbonizing the u.s. electricity sector," tech. rep., National Renewable Energy Laboratory, 2019. Accessed: 2025-03-04.

[51] A. H. Reksten, M. S. Thomassen, S. Møller-Holst, and K. Sundseth, "Projecting the future cost of pem and alkaline water electrolysers; a capex model

including electrolyser plant size and technology development," *International Journal of Hydrogen Energy*, vol. 47, no. 90, pp. 38106–38113, 2022.

[52] H. Lange, A. Klose, W. Lippmann, and L. Urbas, "Technical evaluation of the flexibility of water electrolysis systems to increase energy flexibility: A review," *International Journal of Hydrogen Energy*, vol. 48, no. 42, pp. 15771–15783, 2023.

[53] F. Chen, Z. Gao, R. Loutfy, and M. Hecht, "Analysis of optimal heat transfer in a pem fuel cell cooling plate," *Fuel Cells*, vol. 3, pp. 181 – 188, 12 2003.

[54] H. Becker, J. Murawski, D. V. Shinde, I. E. L. Stephens, G. Hinds, and G. Smith, "Impact of impurities on water electrolysis: A review," *Sustainable Energy & Fuels*, vol. 7, no. 5, pp. 1402–1420, 2023. First published on 14th March 2023.

[55] J. Andersson and S. Grönkvist, "Investigation of research needs regarding the storage of hydrogen gas in lined rock caverns," *International Journal of Hydrogen Energy*, vol. 44, no. 23, pp. 11901–11919, 2019.

[56] United States Department of Energy, "Physical Hydrogen Storage," n.d. Accessed: 2025-03-04.

[57] E. Wolf, "Chapter 9 - Large-Scale Hydrogen Energy Storage," in *Electrochemical Energy Storage for Renewable Sources and Grid Balancing* (P. T. Moseley and J. Garche, eds.), pp. 129–142, Amsterdam: Elsevier, 2015.

[58] Vattenfall AB, "Hybrit: Large-scale storage of fossil-free hydrogen gas successfully proven," 27 February, 2025. Accessed: 2025-03-04.

[59] L. Mansson and P.Marion,, "The LRC Concept and the Demonstration Plant in Sweden – A New Approach to Commercial Gas Storage," n.d. Accessed: 2025-03-04.

[60] V. Stenberg, K. Eriksson, S. Heyne, C. Eklöf-Österberg, L. Lindkvist, and N. Ólafur Egilsson, "Slutrapport- Flexibel och robust vätgasproduktion och -lagring i Lysekil," June 2024. Accessed: 2025-03-04.

[61] F. Johansson, J. Spross, D. Damasceno, J. Johansson, and H. Stille, "Investigation of research needs regarding the storage of hydrogen gas in lined rock caverns," 2018. Accessed: 2025-03-10.

[62] M. Masoudi, A. Hassanpouryouzband, H. Hellevang, and R. S. Haszeldine, "Lined rock caverns: A hydrogen storage solution," *Journal of Energy Storage*, vol. 84, p. 110927, 2024.

[63] A. S. Mehr, A. D. Phillips, M. P. Brandon, M. T. Pryce, and J. G. Carton, "Recent challenges and development of technical and technoeconomic aspects for hydrogen storage, insights at different scales; a state of art review," *International Journal of Hydrogen Energy*, vol. 70, pp. 786–815, 2024.

[64] Energistyrelsen, "Technology Data for Energy Storage," n.d. Accessed: 2025-03-04.

[65] A. A. Kebede, T. Kalogiannis, J. Van Mierlo, and M. Berecibar, "A comprehensive review of stationary energy storage devices for large scale renewable energy sources grid integration," *Renewable and Sustainable Energy Reviews*, vol. 159, p. 112213, 2022.

[66] IRENA, "Utility-Scale Batteries Innovation Landscape Brief," 2019. Accessed: 2025-03-04.

[67] IEA Greenhouse Gas RD Program, "Technical Report 2023-04 Components of CCS Infrastructure - Interim CO2 Holding Options," 2023. Accessed: 2025-02-20.

[68] Equinor, "Northern Lights FEED Report," 2020. Accessed: 2025-03-03.

[69] E. GhasemiKafrudi, L. Samiee, Z. Mansourpour, and T. Rostami, "Optimization of methanol production process from carbon dioxide hydrogenation in order to reduce recycle flow and energy consumption," *Journal of Cleaner Production*, vol. 376, p. 134184, 2022.

[70] N. Meunier, R. Chauvy, S. Mouhoubi, D. Thomas, and G. De Weireld, "Alternative production of methanol from industrial CO2," *Renewable Energy*, vol. 146, pp. 1192–1203, 2020.

[71] P. Baldwin, "Capturing CO2: Gas Compression vs. Liquefaction," June 2009. Accessed: 2025-03-25.

[72] W. X. Meng, S. Banerjee, X. Zhang, and R. K. Agarwal, "Process simulation of multi-stage chemical-looping combustion using aspen plus," *Energy*, vol. 90, pp. 1869–1877, 2015.

[73] A. Razak, "2 - Thermodynamics of gas turbine cycles," in *Industrial Gas Turbines* (A. Razak, ed.), pp. 13–59, Woodhead Publishing, 2007.

[74] K. Lauri, R. Jouko, N. Nicklas, and T. Sebastian, "Scenarios and new technologies for a north-european co2 transport infrastructure in 2050," *Energy Procedia*, vol. 63, pp. 2738–2756, 2014. 12th International Conference on Greenhouse Gas Control Technologies, GHGT-12.

[75] Thunder Said Energy, "Storage Tank Costs: Storing Oil, Energy, Water, and Chemicals," 2023. Accessed: 2025-04-04.

[76] M. Fasihi and C. Breyer, "Global production potential of green methanol based on variable renewable electricity," *Energy Environ. Sci.*, vol. 17, pp. 3503–3522, 2024.

[77] V. H. Nguyen, A. Laari, and T. Koiranen, "The effect of green hydrogen feed rate variations on e-methanol synthesis by dynamic simulation," *Chemical Engineering Research and Design*, vol. 212, pp. 293–306, 2024.

[78] L. Santana, G. dos Santos, A. Santos, C. Marinho, A. Bispo, H. Villardi, and F. Pessoa, "Evaluating the economic influence of water sources on green hydrogen production: A cost analysis approach," *International Journal of Hydrogen Energy*, vol. 89, pp. 353–363, 2024.

[79] N. Mattsson, "Globalenergygis," 2023. Accessed: 2025-04-23.

[80] Electricity Maps, "SE-SE3 Dataset," 2025. Accessed: 2025-04-03.

[81] Decarbonisation Technology, "Conversion of CO2 to Methanol," 2025. Accessed: 2025-03-18.

[82] Energidata Service, "Elspot prices dataset," 2025. Accessed: 2025-04-03.

[83] Christoph Kost and Paul Müller and Jael Sepúlveda Schweiger and Verena Fluri and Jessica Thomsen, "Levelized cost of electricity renewable energy technologies," July 2024. Accessed: 2025-03-04.

[84] Government of Sweden, "Sweden's carbon tax," 2025. Accessed: 2025-03-18.

[85] Practical Law, "Glossary: Discount Rate (US)," 2025. Accessed: 2025-03-18.

[86] M. Shen, L. Tong, S. Yin, C. Liu, L. Wang, W. Feng, and Y. Ding, "Cryogenic technology progress for CO2 capture under carbon neutrality goals: A review," *Separation and Purification Technology*, vol. 299, p. 121734, 2022.

[87] P. Schühle, M. Schmidt, L. Schill, A. Riisager, P. Wasserscheid, and J. Albert, "Influence of gas impurities on the hydrogenation of co2 to methanol using indium-based catalysts," *Catal. Sci. Technol.*, vol. 10, pp. 7309–7322, 2020.

[88] R. Brodersen, F. Joensen, and A. D. Jensen, "System and method for removing impurities from CO_2-rich gas streams," 2024. Accessed: 2025-03-25.

[89] S. W. Lovseth, "Gas or liquid: New co_2 mixture property knowledge needed for efficient and robust ccs," 2016. Published: 6 Jan 2016; Last edited: 16 Apr 2025; Accessed: 22 May 2025.

[90] Mareld Green Energy AB, "Teknisk Beskrivning Mareld Vindkraftpark," 2023. Accessed: 2025-03-04.

[91] Concawe, "E-fuels: A techno-economic assessment of european domestic production and imports towards 2050 – update," 2024. Accessed: 2025-03-11.

[92] S. Mbatha, X. Cui, P. G. Panah, S. Thomas, K. Parkhomenko, A.-C. Roger, B. Louis, R. Everson, P. Debiagi, N. Musyoka, and H. Langmi, "Comparative evaluation of the power-to-methanol process configurations and assessment of process flexibility," *Energy Adv.*, vol. 3, pp. 2245–2270, 2024.

[93] Göteborg Energi, "Kapacitetsutmaningen." `https://www.goteborgenergi.se/om-oss/vad-vi-gor/hallbarhet/kapacitetsutmaningen`, 2024. Accessed: 2025-05-13.

[94] International Renewable Energy Agency, *Renewable power generation costs in 2023*, September 2024. Accessed: 2025-03-10.

[95] European Hydrogen Observatory, *Manual – Levelised Cost of Hydrogen (LCOH) Calculator*. Clean Hydrogen Joint Undertaking, June 2024. Accessed: 2025-03-10.

[96] European Commission, Clean Hydrogen Observatory, "Cost of hydrogen production," 2025. Accessed: 2025-03-10.

[97] International Energy Agency, *Global Hydrogen Review 2023*, December 2023. Accessed: 2025-03-10.

[98] S. Chatterjee, R. K. Parsapur, and K.-W. Huang, "Limitations of ammonia as a hydrogen energy carrier for the transportation sector," *ACS Energy Letters*, vol. 6, no. 12, pp. 4390–4394, 2021.

[99] Lux Research, "Future of methanol: The cost of moving away from natural gas," 15 August 2024. Accessed: 2025-03-13.

[100] James Chen, "Risk Discount: What It is, How It Works, Examples," 2022. Accessed: 2025-05-19.

[101] Jason Fernando, "Net Present Value (NPV): What It Means and Steps to Calculate It," 2024. Accessed: 2025-05-19.

[102] The Engineering Toolbox, "Gases - specific heat and individual gas constants," 2003. Accessed: 2025-03-27.

[103] Air Supply UK, "A guide to air compressor efficiency: how to calculate and maximise efficiency," 2023. Accessed: 2025-03-27.

[104] The Engineering Toolbox, "Higher calorific values of common fuels: Reference data," 2004. Accessed: 2025-03-27.

[105] N. Mattsson, V. Verendel, F. Hedenus, and L. Reichenberg, "An autopilot for energy models – automatic generation of renewable supply curves, hourly capacity factors and hourly synthetic electricity demand for arbitrary world regions," *Energy Strategy Reviews*, vol. 33, p. 100606, 2021.

[106] Vestas Wind Systems A/S, "V236-15.0 MW™ Offshore Wind Turbine," 2021. Accessed: 2025-04-24.

[107] J. F. Casabella and Y. Chehade, "Feasibility study of implementing Chemical Looping Combustion with BECCS: Process modeling and techno-economic analysis of a CHP plant at Skövde Energi," master's thesis, Chalmers University of Technology, Gothenburg, Sweden, 2023.

A

Compression work

Table A.1: Parameter values and result from H_2 compression calculations

Parameter	**H_2 Tank**	**H_2 LRC**	**Unit**	**Source**
P_2	200	250	bar	-
k_{H_2}	1.405	1.405	-	[102]
η_{is}	0.75	0.75	-	[103]
C_{p,H_2}	14.32	14.32	kJ/kgK	[102]
LHV_{H_2}	0.0333	0.0333	MWh_{H_2}/kg_{H_2}	[104]
W	0.0409	0.0474	MWh/MWh_{H_2}	-

B

Wind Data

Niclas Mattsson, Senior Research Engineer at Chalmers University of Technology, generated the wind data used in this project through a model called GlobalEnergyGis, which is a model created by Mattsson himself, Verendal, Hedenus, and Reichenberg that can generate renewable energy data for energy models using public datasets for arbitrary regions all over the world [105]. The region where Mareld is planned to be installed, as well as the generated wind data used in the model is illustrated in Figure B.1, where the location of the Lysekil refinery is marked with a blue dot.

(a) Location of Mareld

(b) Generated wind data region

Figure B.1: Illustrations of the Mareld wind farm region and corresponding wind data region.

In this thesis, the data has been adjusted to offshore floating wind turbines to align with Marelds specifications. The wind data have been taken at 200 meters above sea level and stretch from 1980 to 2019, where 2019 has been chosen as the reference year for the analysis.

The power curve has been determined by assuming the specifications from Vestas V-236 15 MW wind turbine, with a cut-in speed of 3 m/s and a cut-off speed at 31 m/s [106]. It has also been assumed that there are wake and electricity losses. The final power curve for the Mareld wind farm is illustrated and compared with an estimated power curve for the chosen wind turbine in Figure (B.2).

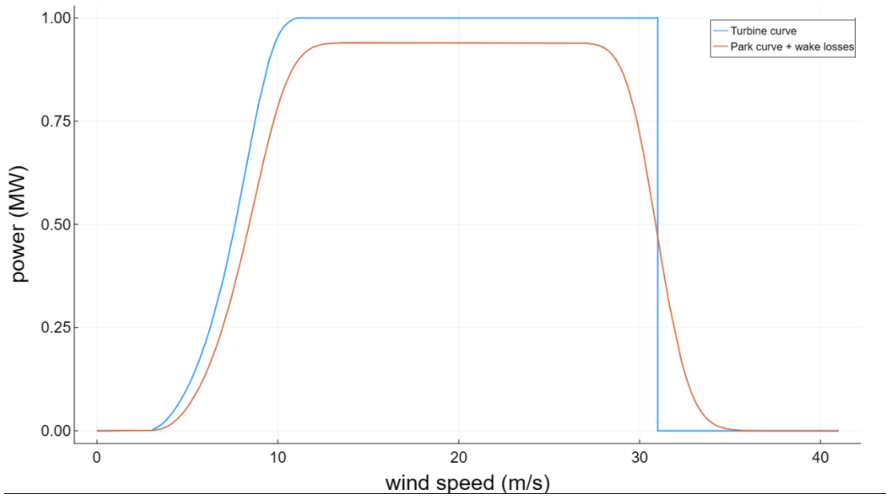

Figure B.2: Power curve for Vestas V-236 15MW wind turbine, assumed to be used at Mareld wind farm.

C

Electrolyzer technologies

Table A.1 presents the input values used for the sensitivity analysis shown in Figure 4.7, where a comparison of the LCOM was performed for different electrolyzer technologies. For the SOEC, a steam demand of 0.2 MWh_{steam}/MWh_{H_2} and a steam cost of 60 €/MWh_{steam} were assumed [64], [107]. Simplifications have been made for the AWE and SOEC regarding additional parameters such as compressor work and surrounding systems. The sensitivity analysis is only to illustrate if the choice of electrolyzer has a large impact on the LCOM. It does not aim to capture the full technical and operational differences between the electrolyzers or the different system setups. For example, did the analysis not take into account the substantially lower operating pressures for AWE and SOEC, resulting in a higher variable OPEX cost.

Table C.1: Parameter values used in sensitivity analysis for different electrolyzers

Parameter	**AWE**	**PEM**	**SOEC**	**Unit**	**Source**
Low η	55	51	85	[%]	[52],[64]
High η	71	68	95	[%]	[52],[64]
Low CAPEX	750	1000	800	[k€/MW]	[Assumption]
High CAPEX	2000	3000	3000	[k€/MW]	[Assumption]
Fixed OPEX	5	5	12	[% of CAPEX/year]	[Assumption]
Minimum load	20	0	0	[%]	[52]
Ramp down rate	100	100	20	[%/h]	[52], [Assumption]
Ramp up rate	100	100	5	[%/h]	[52], [Assumption]

DEPARTMENT OF SPACE, EARTH AND TECHNOLOGY
CHALMERS UNIVERSITY OF TECHNOLOGY
Gothenburg, Sweden
www.chalmers.se

CHALMERS
UNIVERSITY OF TECHNOLOGY